

La 709
5.12
J-2

REPUBLIC OF PERU

74P

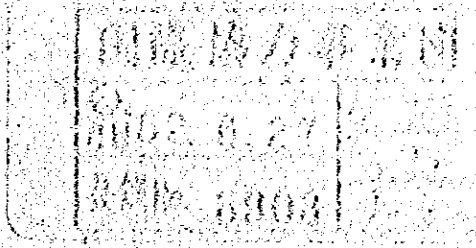
REPORT ON GEOLOGICAL SURVEY
OF THE CORDILLERA ORIENTAL,
CENTRAL PERU

VOL. II



JULY 1976

METAL MINING AGENCY
JAPAN INTERNATIONAL COOPERATION AGENCY
GOVERNMENT OF JAPAN



国際協力事業団	
受入 月日	'84.3.23
	709
	66.1
登録No.	Q1767
	NP

PREFACE

The Government of Japan, in response to the request of the Government of the Republic of Peru, decided to conduct a geological survey for mineral exploration in central part of Cordillera Oriental of Peru, and commissioned its implementation to the Japan International Cooperation Agency.

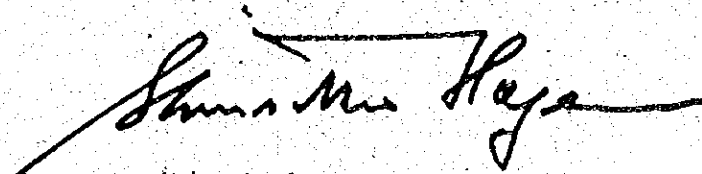
The Agency, taking into consideration of the importance of technical nature of the survey work, in turn sought the Metal Mining Agency of Japan for its cooperation to accomplish the task within a period of four years.

This year was for the first phase survey, and as for this current year, a survey team was formed consisting of six (6) members headed by Mr. Shigeaki Yoshikawa, Mitui Kinzoku Engineering Service Co., Ltd., and sent to the Republic of Peru on September 2, 1975. The team stayed there for seventy-one (71) days from September 2, 1975 to November 14, 1975. During the period of its stay, the team, in close collaboration with the Government of the Republic of Peru and its various authorities, was able to complete survey works on schedule.

This report submitted hereby summarizes the results of the Geological-Geochemical Precisely performed for the first-phase and second phase survey, and it will be also formed a portion of the final report that will be prepared with regard to the results obtained in the second, the third and the fourth phases.

I wish to take this opportunity to express my heartfelt gratitude to the Government of the Republic of Peru and the other authorities concerned for their kind cooperation and support extended to the Japanese survey team.

July 1976



Shinsaku Hogen
President
Japan International Cooperation
Agency

**Geological Geochemical Precise Survey
in the San Vicente Area**

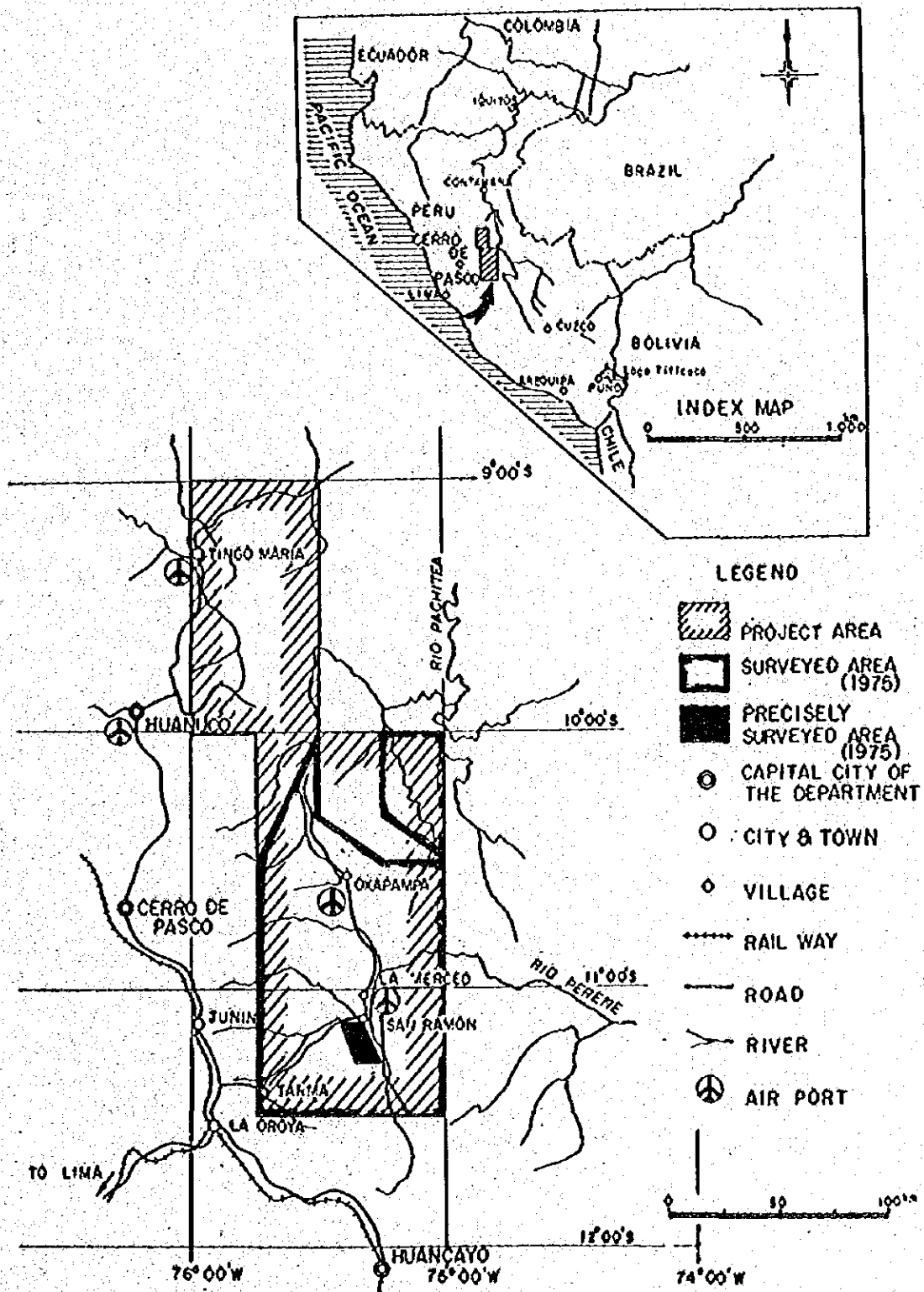


Fig. C-1 Location Map of the Precisely Surveyed Area

CONTENTS

Geological Geochemical Precise Survey in the San Vicente Area

LIST OF ILLUSTRATIONS	3
LIST OF TABLES	4
LIST OF PLATES (in the associated case)	4
Chapter 1. Brief Summary of Works	5
1-1. Purpose of Survey	5
1-2. Field Operation	5
1-3. Indoor Works	6
Chapter 2. Geographical Environment	8
2-1. Location and Accessibility	8
2-2. Climate and Vegetation	9
2-3. Topography	10
Chapter 3. Geology	11
3-1. General Summary	11
3-2. Stratigraphy	11
3-3. Igneous Rock	14
Chapter 4. Geological Structure and History	17
4-1. Folding and Faulting Structures	17
4-2. Geological History	19

Chapter 5. Geology of Ore Deposits	21
5-1. San Vicente Ore Deposit	21
5-2. Alteration of Carbonate Rocks as related to Mineralization	27
5-3. Geochemical Survey	30
Chapter 6. Conclusion and Future Aspects.	41
6-1. Conclusion	41
6-2. Exploration Methods for Future	42
6-3. Future Aspects	43

LIST OF ILLUSTRATIONS

- Fig. C-1 Location Map of the Precisely Surveyed Area
- Fig. C-2 Schematic Geological Profile of the Precisely Surveyed Area
- Fig. C-3 Structural Map of the Precisely Surveyed Area
- Fig. C-4 Schematic Geological Profile of the San Vicente Mining District
- Fig. C-5 Partial Sketch of the Outcrop, the San Vicente Ore Body
- Fig. C-6 Analytical Map of the carbonaceous rocks by X-ray diffraction
- Fig. C-7 Comparative diagrams between the X-ray data and geology along the Mine Road, San Vicente
- Fig. C-8 Partial Sketch of the Vein near the Siete Jeringas Ore Body
- Fig. C-9 Summarized Map of the Geochemical Data of Precisely Surveyed Area
- Fig. C-10 Histograms and Frequency Diagrams of Cu-Zn-Pb (Stream Sediments)
- Fig. C-11 Histograms and Frequency Diagrams of Cu-Zn-Pb (Soils)
- Fig. 6-A Contoured Map of S-Element in Carbonate Rocks
- Fig. 6-B Contoured Map of Zn-Element in Carbonate Rocks
- Fig. 6-C Contoured Map of S/Zn in Carbonate Rocks

LIST OF TABLES

- Table C-1 Generalized Geological Column of Precisely Surveyed Area
- Table C-2 The List of Illustrative Tabulation of X-ray diffractive results
- Table C-3 Charts of X-ray Diffractive Analysis
- Table C-4 Flow Sheets of Geochemical Analysis
- Table C-5 Chemical Data of Selected Samples on 8 Elements
- Table C-6 Statistical Analysis of 8 Elements in Selected Geochemical Samples
- Table C-7 Geochemical Data of the Precisely Surveyed Area on 3 Elements
- Table C-8 Statistical Analysis of 3 Elements of Geochemical Samples in the Precisely Surveyed Area

LIST OF PLATES (in the associated case)

- PL. C-1. Route Map of the Precisely Surveyed Area.
- PL. C-2. Geological Map of the Precisely Surveyed Area.
- PL. C-3. Geological Profile of the Precisely Surveyed Area.
- PL. C-4. Locality Map of Geochemical Sample.
- PL. C-5. Geochemical Map of the Precisely Surveyed Area. (3 sheets)

Chapter 1 Brief Summary of Works

As it has been stated at the very beginning of Chapter 2, Vol. II of the report, the operations of present geological survey of the Cordillera Oriental, Central Peru, consists of the geological geochemical reconnaissance survey in the southern block of the entire projected area (the A and B Areas) and the geological geochemical precise survey in the San Vicente area. This section of the report, Vol. I, deals with the reports and comments on the precise survey in the San Vicente Area, which covers about 100 square kilometers in the southern part of the projected area and includes the San Vicente Mine, presently under active operation.

1-1 Purpose of Survey

The purpose of the precise survey was to make clear the situation and distribution of the Pucara Group in the regional geological setup of the area, through the practice of precise geological geochemical survey as well as to establish the most appropriate procedures of exploration for the bedded lead-zinc deposits which are embedded in the Pucara Group and best represented by the San Vicente Deposits in this area.

1-2 Field Operations

1-2-1 Precise Geological Survey

This survey covered the area of about 100 square kilometers including the San Vicente Mine, occupying the southern part of the projected area.

The topographic maps of scale 1/25,000 were used for the present survey, which were issued by the "Oficina Nacional de Reforma Agraria". The transportation was not much facilitated except the surroundings of the San Vicente Mine. The field works were performed from 19th September to

28th October, 1975. The works were performed as scheduled without any serious trouble in spite of some disadvantages due to intermittent showers and consequent sudden increase of stream water which were the extraordinary weather conditions of the year.

1-2-2 Geochemical Survey

This survey was attempted to find out the applicability of this method for the survey of the vast projected area covering 20,000 square kilometers, and the experimental operation was executed in a limited area surrounding the San Vicente Mine, which was the representative ore deposit in the surveyed area. Procedures of sample collection and preparation of assay samples are almost similar to what has been explained in Chapter 9, Vol.II of the report, and will be mentioned in Chapter 5, Vol. I. (cf. 5-3-1)

1-3 Indoor Works

The indoor works were performed as stated below for the investigation of the field data of geochemical samples.

1-3-1 Geochemical Analysis and Data Analysis

Eight elements were analyzed by the atomic absorption method on the 40 samples randomly extracted from all the geochemical samples of 412, and through the investigation of the assay results, the rest were analyzed for the three elements of Cu, Zn, and Ni, as the three were found effective for the survey of ore deposits as indicators.

1-3-2 X-ray Diffraction

The investigations by the X-ray diffraction method were done on 53 samples to clarify the wall rock alteration caused by the formation of the San Vicente Ore Deposit and on another six samples for the identification of minerals.

1-3-3 Photogeologic Interpretation

Photogeologic interpretation was tried to make clear the geological structures in and around the San Vicente Area.

1-3-4 Examination of Fluid Inclusions

The filling temperatures of fluid inclusions in the host rocks of the San Vicente Deposits were measured to aid for the genetical consideration of the deposits.

Chapter 2 Geographical Environment

2-1 Location and Accessibility (Fig. C-1)

The San Vicente Area is located in the sub-Andean highland of the central part of the Republic of Peru, stretching approximately 100 square kilometers and occupying the southern part of the entire projected area of the present survey. The area is involved in the administrative district of Distrito Chanchamayo, Provincia Tarma, Departamento Junin.

The San Vicente Mine, being in the center of the Area, is located at $11^{\circ} 09'$ south latitude and $75^{\circ} 18'$ west longitude.

The land transportation is widely used to access to the surveyed area, as there are many facilities, such as regular bus services from Lima, the domestic airline makes regular flight once a week between the two.

National Highway 20A	National Highway 20B
Lima-----La Oroya-----	-----San Ramon-----
187 km, 4 hrs.	121 km, 3 hrs.
Local Highway	
-----San Vicente	
18 km, 50 min.	

The National Highway 20A is almost perfectly paved, double laned road, while 20B is paved and double laned only for about half way and the rest is unpaved and partly single laned. The National Highway 20A passes through Tielio Pass, 4843 m SL., on its closer approach to Oroya. Both highways have to pass through the steep slopes on each side of the Pass following the valleys.

The transportation facilities are generally poor in the surveyed area except the vicinity of the San Vicente Mine.

The transportation between the San Vicente Mine and San Ramon, main community of this district, is facilitated by the regular bus services.

2-2 Climate and Vegetation

The area belongs to the subtropical climatic zone with high temperature and high humidity, but the western subhighland has more or less the climate of tropical highland. This district has no climatic change of four seasons, but has dry and rainy seasons. It has been said that the dry season continues from April to September and the rainy season from October to March next year, but in the western subhighland, the dry season lasts about one month longer to October. Fine weather continues day by day especially during the period from July to August. It rains almost every day during the rainy season, and sometimes the rainfall exceeds 100 mm in a day. Clouds are abundant even in the dry season, but causing only occasional showers of a little amount. The temperature of the dry season has so big a difference in day and night, as the average is 28°--30° C at daytime max., while 13°--14° C in the night. The temperature during the rainy season is a little less than the dry season either in the day or night.

The thick vegetation of mostly of broad leaf trees covers the area widely, but the mountain skirts are mostly cultivated for plantation of fruits such as bananas, pineapples, and papayas. In the western subhighland is spread vastly the grass field, in which the patches along the valleys are cultivated for the plantation of eucariptus trees and the flat fields for pasturage.

2-3 Topography

The area occupies the western terminal of a basinlike topography intersticed between the Andes and Sub-Andes, which forms the front of the Eastern Andes, having the lowest altitude of about 950 meters in the northeastern corner and the highest of about 2,700 meters in the western end. The main streams are the Rio Tulumayo, which flows from south to north in the eastern end of the area, and the Rio Aynamayo, which flows southwest towards northeast of the area and joins to the Rio Tulumayo. The river terraces are well developed along the downstream from the vicinity of the junction of the two streams, and talus deposits are also developed between the terraces and the steep slopes of backyard highlands. The V-shaped valleys are well developed in the granitic terrains of the east and west of the area to form the wedge like summits, while the stream system displays the typical dendritic pattern where the terrain has no effects of tectonic lines or faults. In the central limestone area, the U-shaped valleys are developed, leaving flats on top of the highland, and the main stream courses are controlled by tectonic lines. The topography is much more gentle in the area of sandstone and conglomerate, which is the west annex to the limestone area, as they are less resistant for erosion. There are three stages of the river terraces along the main streams of the Rio Tulumayo and Rio Tarma, and are cultivated for agricultural products and fruit tree plantation.

Chapter 3 Geology

3-1 General Summary (Table C-1 and Fig. C-2)

The geological setup of the San Vicente Area may roughly be summarized as follows.

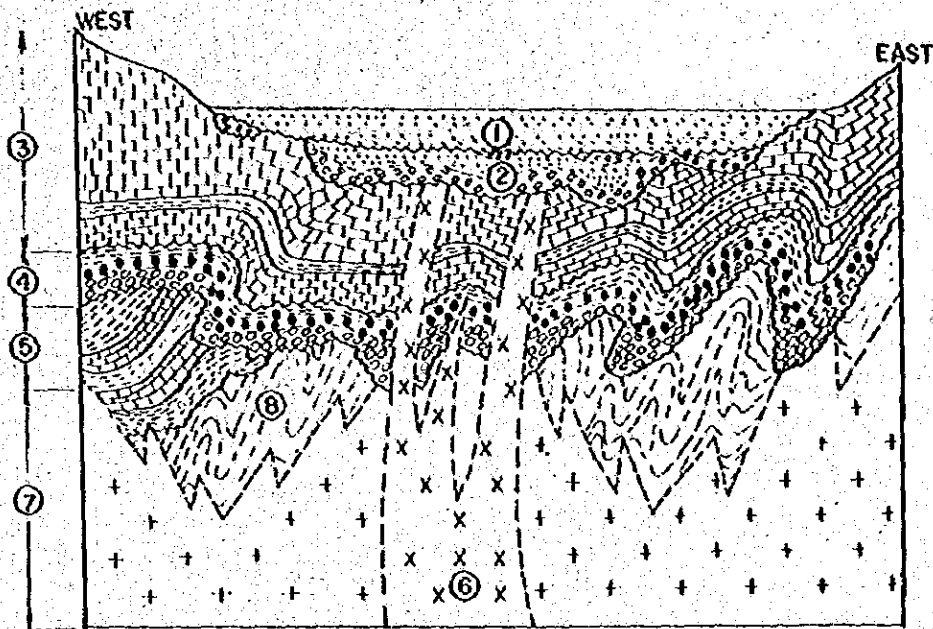
The sediments after middle Permian occupy vastly the central part of the area, which consist of the layers of red shale and sandstone of the Mitu Group, and those of limestone and dolomite of the Pucara Group, while the older intrusive bodies of granite and granodiorite that are considered to constitute the basement complex, are distributed in the east and west sides of the sedimentary area. And in the northwestern and southern parts of the area, the younger intrusives are exposed as stocks of small scale, penetrating the Mitu and Pucara Groups. Further, the Quaternary sand and gravel beds are covering them partially. To the south of the area, Pre-Cambrian metamorphosed rocks consisting of gneiss and crystalline schist are distributed, and the sedimentary rock to be considered Taruma formation was found as the xenolith.

3-2 Stratigraphy



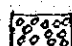



The stratigraphy of the area consists of the Mitu Group of middle or upper Permian, the Pucara Group of middle Triassic or lower Jurassic, and the Quaternary sand and gravel beds.

3-2-1 Mitu Group

This formation has a wider distribution from north to south of the area, which is mainly composed of the layers of reddish brown lutite, and fine sandstone, accompanying well stratified limestone and limestone conglomerate as well as pyroclastics and andesite lava flows.



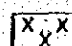


SEDIMENTARY ROCKS

-  SAND, CLAY & GRAVEL
-  SANDSTONE
-  CONGLOMERATE
-  LIMESTONE CONGLOMERATE
-  LUTITE & SHALE
-  LIMESTONE

GEOLOGICAL UNITS

- ① ALLUVIUM TALUS ETC. (RECENT)
- ② PARACAS FORMATION (TERTIARY EOCENE)
- ③ PUCARA GROUP (TRIASSIC ~ JURASSIC)
- ④ MITU GROUP (PERMIAN ~ TRIASSIC)
- ⑤ TARMA GROUP (CARBONIFEROUS)

INTRUSIVE ROCKS

-  DIORITE COMPLEX → ⑥ (CRETACEOUS ~ TERTIARY)
-  GRANODIORITE & GRANITE → ⑦ (PERMIAN)
-  GNEISS & SCHIST → ⑧ (PRE-CAMBRIAN)

 UNCONFORMITY

Fig. C-2 Schematic Geological Profile of the Precisely Surveyed Area

Table C-1 Generalized Geological Column of Precisely Surveyed Area

AFTER BELLIDO, E. (1969)
LEVIN, M. & SAMANIEGO, A. (1975)

GEOLOGICAL AGE		GEOLOGICAL UNITS	COLUMNAR SECTION	IGNEOUS ACTIVITY	DESCRIPTIONS				
CENOZOIC	QUATERNARY	HOLOCENE		DIORITE COMPLEX	GRAVEL, SAND & CLAY				
		PLEISTOCENE			DILUVIUM				
	TERTIARY	PLIOCENE			UPPER PART : SANDSTONE WITH CONGLOMERATE LOWER PART : CONGLOMERATE WITH SANDSTONE				
		MIOCENE							
		OLIGOCENE							
		EOCENE							
		PALAEOCENE							
MESOZOIC	CRETACEOUS			DIORITE COMPLEX	CENTRAL PART : TONALITE & GRANODIORITE MARGINAL PART : DIORITE				
		JURASSIC				LATER			
	JURASSIC	MIDDLE							
	JURASSIC	EARLIER							
	TRIASSIC	LATER							
		MIDDLE							
		EARLIER							
	PERMIAN	LATER				MITU GROUP		DIORITE COMPLEX	UPPER PART : SANDSTONE & LUTITE WITH CONGLOMERATE MIDDLE PART : LIMESTONE CONGLOMERATE WITH LUTITE LOWER PART : CONGLOMERATE WITH LUTITE
		MIDDLE							
		EARLIER							
PALAEOZOIC	CARBONIFEROUS	LATER		DIORITE COMPLEX	GREY TO BLACK LUTITE WITH THIN BEDS OF LIMESTONE				
		EARLIER							
	DEVONIAN		DIORITE COMPLEX		EASTERN PART : RED GRANITE WITH GREY GRANODIORITE WESTERN PART : GREY GRANODIORITE				
	SILURIAN								
	ORDOVICIAN								
CAMBRIAN	BASAL COMPLEX		DIORITE COMPLEX	GNEISS & SCHIST					
PRE-CAMBRIAN									

LEGEND

SEDIMENTARY ROCK

- SAND
- GRAVEL
- LUTITE, SHALE & PHYLLITE
- SANDSTONE
- CONGLOMERATE
- LIMESTONE

METAMORPHIC ROCK

- GNEISS & SCHIST

IGNEOUS ROCK

- DIORITE
- GRANITE

This formation, except limestones, has generally an outstanding reddish tone by which the formation is characterized. The total thickness of it is estimated 2,000 meters more or less.

(1) Lutite and Fine Sandstone

Most of the Mitu Group is composed of lutite and fine sandstone. They are reddish brown and soft rocks, and they are so feeble against weathering and erosion, easily decomposed into soils, that the fresh exposures of them are very scarce. This makes it impossible to ascertain the definite relations with the overlying Pucara and underlying Mitu Groups.

(2) Limestone Conglomerate

In this area, this limestone conglomerate sits on the upper part of the Mitu Group forming a horizon marker, of which thickness varies from 60 to 200 meters, thicker and persistent in the north, while thinner and ill persistent in the south. This conglomerate consists of sub-angular pebbles of 2 or 3 cm in diameter, of which majority is limestone but very few pebbles of granodiorite and reddish brown lutite are accompanied.

(3) Limestone

This can be recognized throughout the distribution of the Mitu Group, but the exposures are very scarce, as the rocks are mostly found in the talus deposits, and consequently the accurate distribution is obliterated. This is a comparatively muddy limestone, well stratified but mostly brecciated. The better exposure of this formation can be seen along the stream of Union Mantos in the central and southern part of the area, where a few layers of 10 to 30 cm thick are interbedded in the reddish lutite.

(4) Pyroclastics and Andesite Lava Flows

This formation occupies the uppermost part of the Mitu Group stratigraphically, lying immediately under the Pucara Group. The andesite

lava flows are represented by a porphyritic andesite of which phenocrysts of feldspar are outstanding. The pyroclastics consist of the cognate breccias. They are commonly reddish purple.

3-2-2 Pucara Group

This formation is widely distributed in the central part of the area, usually causing characteristics steep topography. The Pucara Group may be divided into three formations, namely from the lower upwards, grey limestone, dolomite, and black muddy limestone formations. The thickness of the Group exceeds 1,500 meters but the precisity is obscured as its upper part has been cut off by the thrusting granodiorite.

(1) Grey Limestone

This formation has its typical exposures in the south of Hda. Don Alberto in the north of the area and in the surroundings of Huacrash in the south. It usually consists of well stratified grey or dark grey limestones, occasionally intercalating black shale and grey calcareous fine sandstone. It is difficult to distinguish it from the limestone of the Mitu Group due to the similar lithological appearances of the two. In a small stream south of Hda. Alberto, an exposure of grey limestone contains shell fossils.

(2) Dolomite

It is widely distributed continuously from the Rio Puntayacu Junior in the north to the Rio Siete Jeringos in the south. The rock is grey or dark grey in color with distinct stratification, showing no reaction by dilute hydrochloric acid, or faint reaction if any. Very often the formation is made crystalline, some of which form the Zebra structure with the alternation of thin layers of white and dark grey crystalline dolomites of a few mm or one cm thick. Some of the dark grey layers consist of minute grains of sphalerite.

(3) Black Limestone

This has its typical distribution at the west of the San Vicente Mine on the upstream of Rio Puntayacu and on the upstream of Qda. Agua Blanca in the northern part of the area.

The formation is mainly composed of black and fine sandy limestone or calcareous sandstone with well developed stratification, intercalating greyish brown mudstone. Abundant fossils of Ammonites are found in the mudstone near Uncush Sur, south of San Vicente.

3-2-3 Quaternary Sand and Gravel Beds

There are thick and flat layers of stream or lake sediments of sand, gravel, and clay along the downstreams of Rio Tulumayo and Rio Tarma. Talus deposits are also observed locally on the slopes facing to these main streams.

3-3 Igneous Rocks

The igneous rocks of this area can roughly be divided into the older intrusives of granite and granodiorite constituting the basement complex for the sediments of the Mitu and Pucara Groups, and the younger intrusives of dioritic rocks penetrating both of the said groups.

3-3-1 Granite and Granodiorite

Granite is distributed continuously from north to south along the eastern fringe of the area. It is coarse-grained holocrystalline rock of which orthoclase is mostly pink in color and mafic mineral is biotite. As the rock appears pinkish as a whole, it is called locally 'granito rojo'. This granite often contains the xenoliths of sediments seemingly older than the Mitu Group. But it is practically impossible to ascertain the original rocks, as all of them are metamorphosed into hornfels.

Granodiorite is distributed on the higher parts of the western side of the area. It is white and fine- to medium-grained holocrystalline rock but lacks the pink feldspars. Mafic mineral is biotite. This rock is locally called 'granito blanco' against the 'granito rojo', as it appears white as a whole. This granodiorite contacts with the Pucara Group by faulting, the former having thrust over the limestone formation of the Pucara Group. The faulted relation can be observed clearly on the upstream of the Puntayacu in the west of the San Vicente Mine, where the fault plane is dipping 25° northwest. A sheared zone of about 30 cm thick is formed in the black limestone along the footwall of the fault. Granodiorite of the hangingwall has been altered greenish.

3-3-2 Dioritic Rocks

Exposures are seen near Hda. Alberto, northwest of the area, and near Huacrash in the south of the area, and considering from their distribution they seem to penetrate both the Mitu and Pucara Groups. They have various facies as microdiorite, granodiorite porphyry, and fine-grained granodiorite, but generally speaking they are the intermediate hypabyssal rocks.

(1) Microdiorite is greenish grey hard rock distributed either in the northwest or in the south. The fresh facies exposes at the entrance of a stream named Agua Blanca, where it is greenish grey and hard.

(2) Granodiorite porphyry is light greenish grey, having phenocrysts of quartz and conspicuous feldspar of approximately 5 mm. Mafic minerals are hornblende and biotite. The concentration of the mafic minerals differs in places, and the less mafic portion looks similar to the microdiorite mentioned before. This rock is found either in the northwest or in the south, too.

(3) Fine-grained granodiorite can only be seen as an intrusive body in the east of Huarcash in the south. It is cream colored rock and its acicular mafic minerals are altered greenish.

(4) Pyrite-impregnation of 100 m in diameter is recognized on the western part of the stock cropping out in the vicinity of Hda. Don Alberto and in the part occurring micro-diorite in the vicinity of Huacrash, the former includes copper-calcite vein 5 - 10 cm in width.

Chapter 4 Geological Structure and History

4-1 Folding and Faulting Structures

The asymmetrical foldings with east dipping axial planes, and the west dipping reverse faults cutting off the folding structures, are developed in the region covering the east of the Eastern Andes, or covering from the Andes to the Amazonian Plains through Sub-Andes.

The San Vicente Area is divided into three geological blocks, the northern, central, and southern blocks as shown on Fig. C-3.

The northern block is situated in the west of N-S fault, where the Pucara Group forms the eastern wing of the synclinal structure extending in NNW-SSE.

In the central block, the Pucara Group is distributed as a part of the syncline extending in NNE-SSW. The axis of the syncline is plunging gently towards SSW, and turned gradually into N-S, but as the west part of the syncline is thrust over by a fault of N-S direction, the east wing of the structure alone is remained near the San Vicente Mine, presenting a simple monoclinial structure with north-southward strikes and westward dips. In the east of the block, the structure is cut by the fault of NNE-SSW trend, having the strike and dip nearly similar to those of the Pucara Group. Therefore in the central block, the dolomite of the intermediate horizon is left perfectly, while the limestone layers of the upper and lower seated are only left partially.

The southern block is located in the south of the NE-SW fault and is intruded by the dioritic rocks, which caused some disorder of strikes and dips of the Pucara Group, though the regional trend is N-S in strike with westward dips. In this block, the lower seated limestone

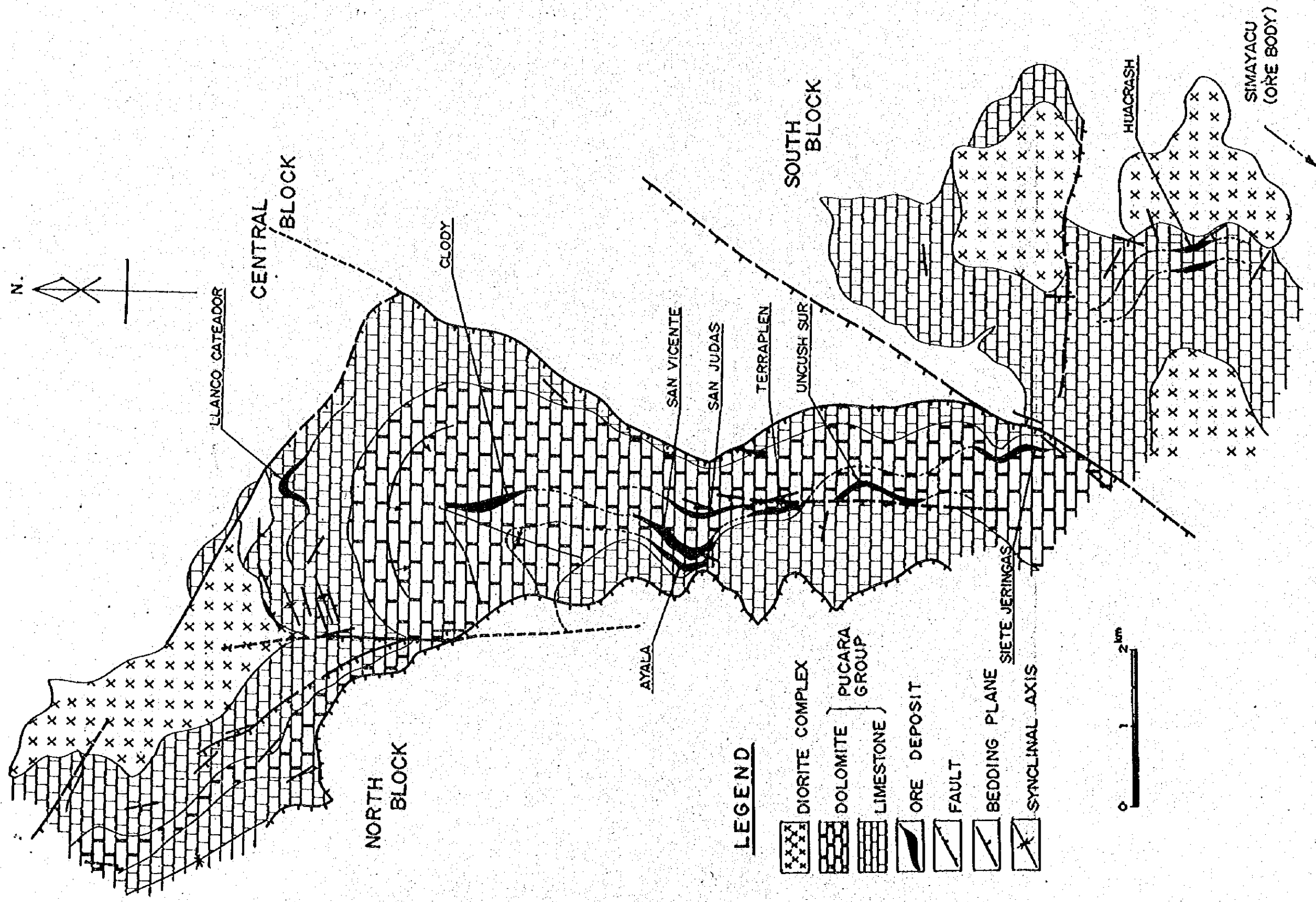
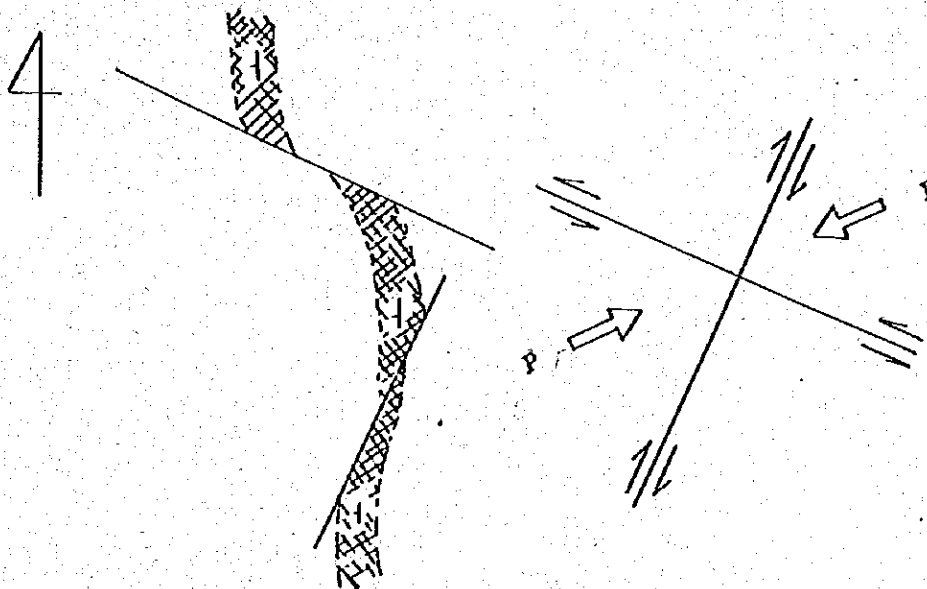


Fig. C-3 Structural Map of Precisely Surveyed Area

layer is only present.

The intrusion of dioritic rocks are controlled by a great synclinal structure extending in NNW-SSE in the central part of the surveyed area macroscopically, as their stocks are scattered parallelly to NNW-SSE, the direction of the syncline. They seem to be partly related to the fissures of E-W and WNW-ESE systems.

The ore body of the San Vicente Mine is cut by the fissures of WNW-ESE and NNE-SSW systems after the mineralization, in which the former is dominant, giving such dislocations as shown below.



It may be understood that this structural pattern of the ore body being cut into pieces were caused by the fissures generated by the lateral compression of ENE-WSW.

The fundamental tectonic lines are patterned by the overthrusts generated by the said lateral compression and resultant fissure systems of WNW-ESE and NNE-SSW. The lateral compression in ENE-SWS direction which generated these tectonic lines might have been due to the Andean

orogeny, which took place in the late Cretaceous or early Tertiary, as the dioritic rocks are dislocated by the fissures of WNW-ESE system.

4-2 Geological History

The oldest formation in the area is a series of metamorphic rocks produced through the sedimentation and orogenies in Pre-Cambrian of Early Paleozoic Era. After the repeated transgressions and regressions and twice of orogenic movements till early Carboniferous Period, there took place a great transgression in which the lutite and limestone of the shell-fossiliferous Tarma formation was deposited. The submarine deposition was ceased at the commencement of the orogenic movement in the middle of Permian Period. The molasses of the Mitu Group were performed later on, in the basins and depressions by the deposition of the materials derived from the erosion of mountains and the debris of volcanic materials.

The ages of intrusion of the granitic rocks constituting the basement complex in the area were determined by K-Ar method in the present operation to have ranged from middle Permian to late Triassic, as stated in Chapter 5, Vol. II of the report. Besides, the age determination on the basal pebbles of the Mitu Group, probably originated from the granitic rocks, has indicated 238 ± 16 m.y.

A geosyncline was formed in the middle or late Triassic Period of Mesozoic Era, and the calcareous sediments of the Pucara Group were deposited there. After the repeated up-and-down movements of the lands, the upheaval was caused by the Andean Orogeny in the late Cretaceous Period in which the dioritic rocks intruded. This magmatic activity is said to have lasted till about Eocene Epoch.

The Paracas formation near San Ramon, mainly composed of the lake sediments, was deposited about the time when the Andean Orogeny had nearly come to its end.

Chapter 5 Geology of Ore Deposits

5-1 San Vicente Ore Deposit (Figs. C-4 and C-5)


5-1-1 General Remarks

The San Vicente Mine is located about the centre of the area of precise survey. The mine is under the operation of Cia. Minera San Ignacio de Morococha S.A. as of October 1975, a company of the domestic capitals. The mine installations are built on both sides of the upstream of Rio Puntayacu in the east of the deposits. The climate is subtropical with thick vegetations and the topography is steep. The deposits crop out at the altitudes from 1,400 meters to 2,000 meters S.L., and are mostly worked underground and partly by open pits. The bottom level is opened at 1,455 meters S.L. The mine produces 1,200 tons of crude ore per day assaying 12--14 % Zn and 0.8--1.0 % Pb.

5-1-2 General Descriptions of Ore Deposits

As shown on Fig. C-3, many outcrops are known scattered around within 15 kilometers in north and south, in which the mine sits in the center.

They are distributed as follows from the north to the south;

North	Llanco Cateador	Zn, Pb, Ag, Cu	limestone	
	Clody	Zn, Pb, Cu	dolomite	
	San Judas, San Vicente, Ayala	Zn, Pb	"	
	Terraplen	" "	"	
	Uncush Sur	" "	"	
	Siete Jeringas	" "	"	
	Huacrash	Zn, Pb, Cu	limestone	
	South	Sinayacu	Zn, Pb	"

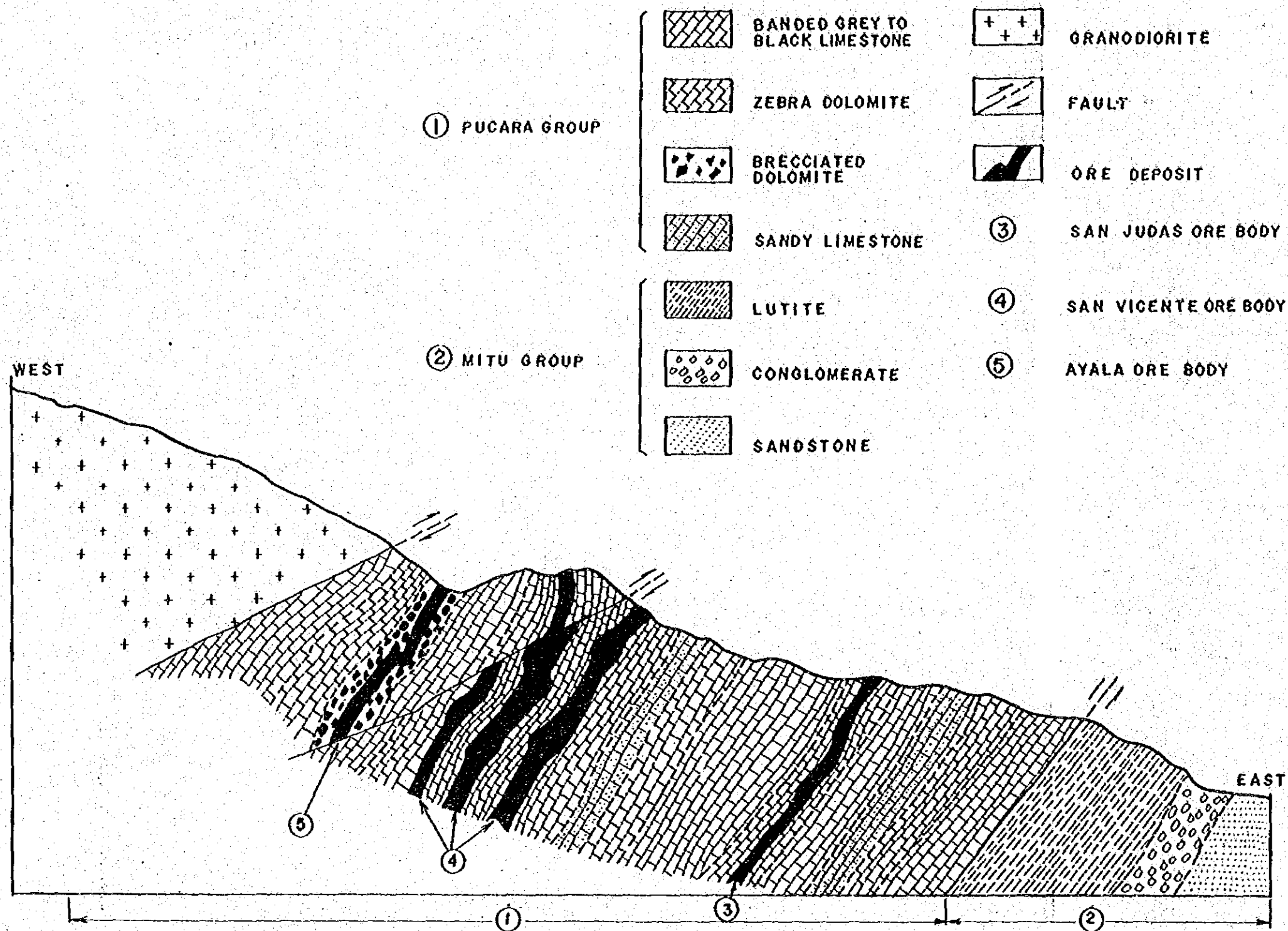


Fig. C-4 Schematic Geological Profile of the San Vicente Mining District

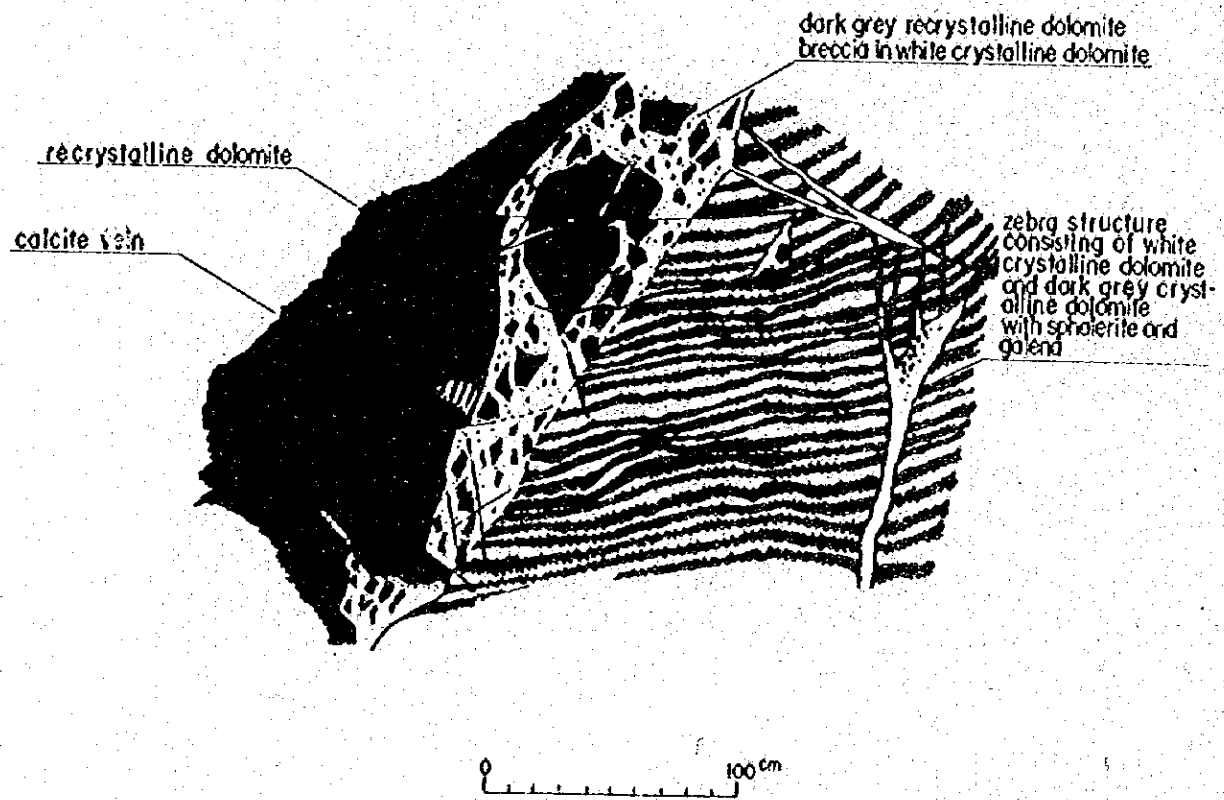


Fig. C-5 Partial Sketch of the Outcrop, the San Vicente Ore Body

Among these ore bodies, the San Vicente Ore Body is most advancedly developed, being the main working object. Others such as San Judas, Ayala, Uncush Sur, Siete Jeringas, are also partly developed. According to Levin, P. (1974), there are 18 ore beds recognized including the uneconomical ones, and 5 beds have been known in the present workings including the San Vicente Ore Body. The following three are the main ore bodies, namely San Judas on footwall side (east), San Vicente in the middle, and Ayala on hangingwall side (west) as shown on Fig. C-3. They are striking almost north-south and dipping westwards. The ore shoots are controlled by folding structures and they are plunging about 40° in northwest.

Followings are the descriptions of the leading ore bodies;

(1) San Judas It is located on the upstream of Rio Puntayacu, occurring as an outcrop of poor lead ore of 6 meters wide, embedded in the banded dolomite of about 50 meters thick. Its downward extension, however, has been developed as assaying averagely 9 % Zn, 13 % Pb with 10 meters width, although its entire extension has not been ascertained.

(2) San Vicente It is located about 500 meters west and on the hanging-wall side of San Judas, which is the main ore body for present working. The ore body is embedded in dolomite and closely related to its banded parts, striking mostly north-south and dipping westwards as 45° -- 50° . It crops out for 900 meters across the Rio Puntayacu. Its southern extremity reaches to the Terraplen Ore Body, and the Clody Ore Body is considered to be embedded in the same horizon.

(3) Ayala Two outcrops have been found and both are embedded in the black limestone. Complicated folding structures are observed in the ore body, but it is considered as a whole to strike in north-south and dipping to west. It has the width of averagely 6 meters, assaying 1% Pb and 14 %

Zn on the outcrop, but its whole dimension has not been ascertained.

(4) **Uncush Sur** This is embedded in the banded dolomite which may be similar horizon to that of San Vicente. The black limestone lies about 40 or 50 meters apart from the hangingwall side of the banded dolomite layer in which the ore body is embedded. The dimension of the ore body has not been clarified yet, but it has a strong possibility to consist of a few metalliferous beds, as the outcrops are scattered for the width of more than 20 meters. The overall assay is not clear though it shows locally as high as 30 % Zn. It strikes nearly north-south with gentle dips of 20°--40°.

(5) **Siete Jeringas** This is also embedded in the banded dolomite which seems similar to that of San Judas. The lower horizon of the ore body is gray banded dolomite, and further below is gray limestone. Although the dimension of the ore body has not been cleared, the outcrop is as wide as 5 to 10 meters. Often massive ore mainly composed of coarse crystals of sphalerite is traversed by the network veinlets of calcite carrying coarse-grained galena (Fig. 8).

5-1-3 Structural and Mineralogical Features of Ore Deposits

The carbonate rocks in the vicinity of the San Vicente Ore Body can be classified stratigraphically as follows;

	Lithology	Ore Bodies
Upper limestone member	Banded black limestone	
Middle dolomite member	Banded black limestone with brecciated dolomite	Ayala
	Crystalline gray dolomite	Clody, San Vicente, Terraplan, Uncush Sur
	Banded gray dolomite with sandy limestone	San Judas, Siete Jeringas
Lower limestone member	Banded gray limestone	Llancó Cateador, Huacrash, Simayacu

As shown on Fig. C-3, the intrusive stocks of the dioritic rocks in the carbonate rocks are observed in the north and south of the area.

There are three metalliferous horizons recognized in the dolomite formation, and the main ore bodies are mostly embedded near the horizon of banded dolomite (Zebra dolomite) seated in the crystalline gray dolomite of the middle dolomite member. The ore bodies are mainly composed of minutely crystalline sphalerite as principal mineral and a small amount of galena.

Pyrite is little in amount and chalcopyrite is much less. There are types of ores of massive, banded, and brecciated, in which the banded ore is most in amount. The banded ore is perfectly concordant to dolomite layers, performing the bandings of 5 to 40 cm in each thickness, in order of gray dolomite, white dolomite, sulphides, white dolomite, and gray dolomite.

The banded structures of ore are roughly divided into three types, namely, massive concentration of sphalerite (Type-A), gangue and sphalerite (Type-B), and gangues only which are repeating the alternations in order of the following combinations;

from the hangingwall side,	gangues only,
	Type-A,
	Type-B,
	Type-A,
	gangues only, and
to the footwall side	Type-A.

Cutting across these bandings, are seen the carbonates-pyrite veins, and sphalerite veins. Such small veins are found more around the faults or fissures. Under the microscope, sphalerite shows massive aggregates of extremely minute crystals in the ore of Type-A and the ore of Type-B is composed of the crystal grains of 0.1--0.2 mm in diameter.

The plunge and folding structure of ore bodies are concordant to such banded structures. There are three kinds of sphalerite in colors, as black, dark brown, and yellowish brown, but the mineralogical investigation such as the difference of composition is not sufficient. Generally speaking, however, the granularity seems to increase in order of black--dark brown--yellowish brown. In the San Vicente Mine, a tendency is noticed that the proportion of color zone increases in this order from the footwall (east) towards the hangingwall (west).

5-1-4 Genesis of Ore Deposits

In view of the parallelism of the ore deposits to the beddings of the layers of Pucara Group, as well as their morphologies and mineral associations, two possibilities have been discussed regarding the genesis of these ore deposits, namely

(1) hydrothermal replacement deposits of low temperature, in which the carbonate rocks of the Pucara Group were replaced by the telemagmatic hydrothermal solutions,

(2) sedimentary ore deposit, of which metallic ions had been dissolved by the anaerobic bacteria and transported during the time of sedimentation of the Pucara Group.

The possibility of the sedimentary origin of the San Vicente Ore Deposits has recently been emphasized because of their concordant relation to the host rocks, long persistency, fine granularity of their ore minerals, lacks of the signs of thermal alterations, and non-existence of igneous rocks as related to the mineralization. On the other hand, it has been suggested necessary through the present survey to restudy the concept of the sedimentary origin or to investigate the migration of ore materials, based upon the following observations;

(1) It has been believed that there has been none of the intrusives related to the genesis of ore deposits in this area, which has been one of the main reasons to support the concept of the sedimentary origin, but the present survey has found the dioritic rocks intruded into the Pucara Group with hydrothermal alteration minerals formed in the surroundings of intrusives.

(2) The galena deposit has been observed among the San Vicente deposits, which is of later formation than the sphalerite deposits. It has utterly irregular form and very often is found intersecting the sphalerite deposits.

(3) The lavas and tuffs commonly observed in the bedded ore deposits related to the submarine volcanism have not been found in the Pucara Group.

Summarizing the facts above stated, a hypothetical interpretation may be performed as follows;

(1) Zinc ions were transported by the anaerobic bacteria during the deposition of the Pucara Group which presently forms the host rock to the ore

deposits. This carrying-in of the Zinc ions was not proceeded uniformly during the course of sedimentation of the Pucara Group, but was locally dominant where the dolomite is presently thicker near the basinal structures.

(2) Along with the accumulation of sediments, the later diagenesis prevailed more in the parts of basinal structures, and zinc ions combined with sulphur ions, which were isolated from the carbonaceous limestone to form sphalerite by the process of diagenesis or others.

(3) The dioritic rocks, enriched themselves with sulphides of heavy metals, intruded from late Cretaceous to early Tertiary Periods, and formed the skarn type ore deposits at the contacts with the carbonate rocks. The hydrothermal solutions derived from the dioritic rocks replaced the carbonate rocks to form the replacement deposits of sphalerite. At the same time, they accelerated the migration of components of pre-existed sphalerite and its re-concentration. Finally the hydrothermal solutions formed the galena veins and pyrite impregnation in the host rocks.

Thus, the bedded zinc-lead deposits of San Vicente type were formed by the superimposed mineralization related to the later magmatic activity over the pre-existed syngenetic deposits, by which the mineral contents have been raised up to the economical grade.

5-2 Alteration of Carbonate Rocks as related to Mineralization (cf. Fig. C-6, C-7, C-8, Table C-2)

Alteration effects of mineralization to the carbonate rocks were examined by X-ray diffraction on 53 samples taken from limestone, muddy limestone, calcareous sandstone, and calcareous shale of the Pucara and Mitu Groups exposed in the San Vicente Mine area.

In this examination, all the conditions except the full scale values

Table C-2 The List of Illustrative Tabulation of X-Ray Diffractive Results

Sample No.	minerals													
		Dolomite	Calcite	Quartz	Barite	Gypsum	Sericite	Chlorite	Plagioclase	Kaolinite	Sphalerite	Smithsonite	Galena	Pyrite
1	H 92004													
2	H 92005													
3	H 92007													
4	H 92105													
5	H 92201													
6	H 92202													
7	H 92203													
8	H 92204													
9	H 92205													
10	H 92206													
11	H 92301													
12	H 10101													
13	H 10102													
14	H 10103													
15	H 10104													
16	H 10105													
17	H 10501													
18	H 10502													
19	H 10503													
20	H 10701													
21	H 10901													
22	H 10902													
23	H101001													
24	H101002													
25	H101101													
26	H101102													
27	H101305													
28	H101401													
29	H101402													
30	H101403													
31	H101404													
32	H102301													

Sample No.	minerals													
		Dolomite	Calcite	Quartz	Barite	Gypsum	Sericite	Chlorite	Plagioclase	Kaolinite	Sphalerite	Smithsonite	Galena	Pyrite
33	H102302													
34	H102303													
35	H102401													
36	H102801													
37	H 102802													
38	H 102804													
39	H 102806													
40	H 102807													
41	H102808													
42	H 102809													
43	H102810													
44	H102811													
45	H102812													
46	H 102813													
47	H 102814													
48	H 102815													
49	H 102816													
50	H 102817													
51	H 102818													
52	H 102819													
53	H 102820													
54	H101103#1													
55	H101303#2													
56	H102803#3													
57	H 92201#4													
58	H 92202#4													
59	H 92203#4													
60	H 92204#4													
61	H 10501#5													
62	H 102301#6													

- #1 : altered andesite
- #2 : altered micro diorite
- #3 : ore (in dolomite)
- #4 : oxidized vein. refer to Fig. C-8
- #5 : oxidized vein.
- #6 : fault clay

- ⊙ Very abundant
- Abundant
- Common
- Few
- Rare

The other samples are all carbonaceous rocks for x-ray analysis.

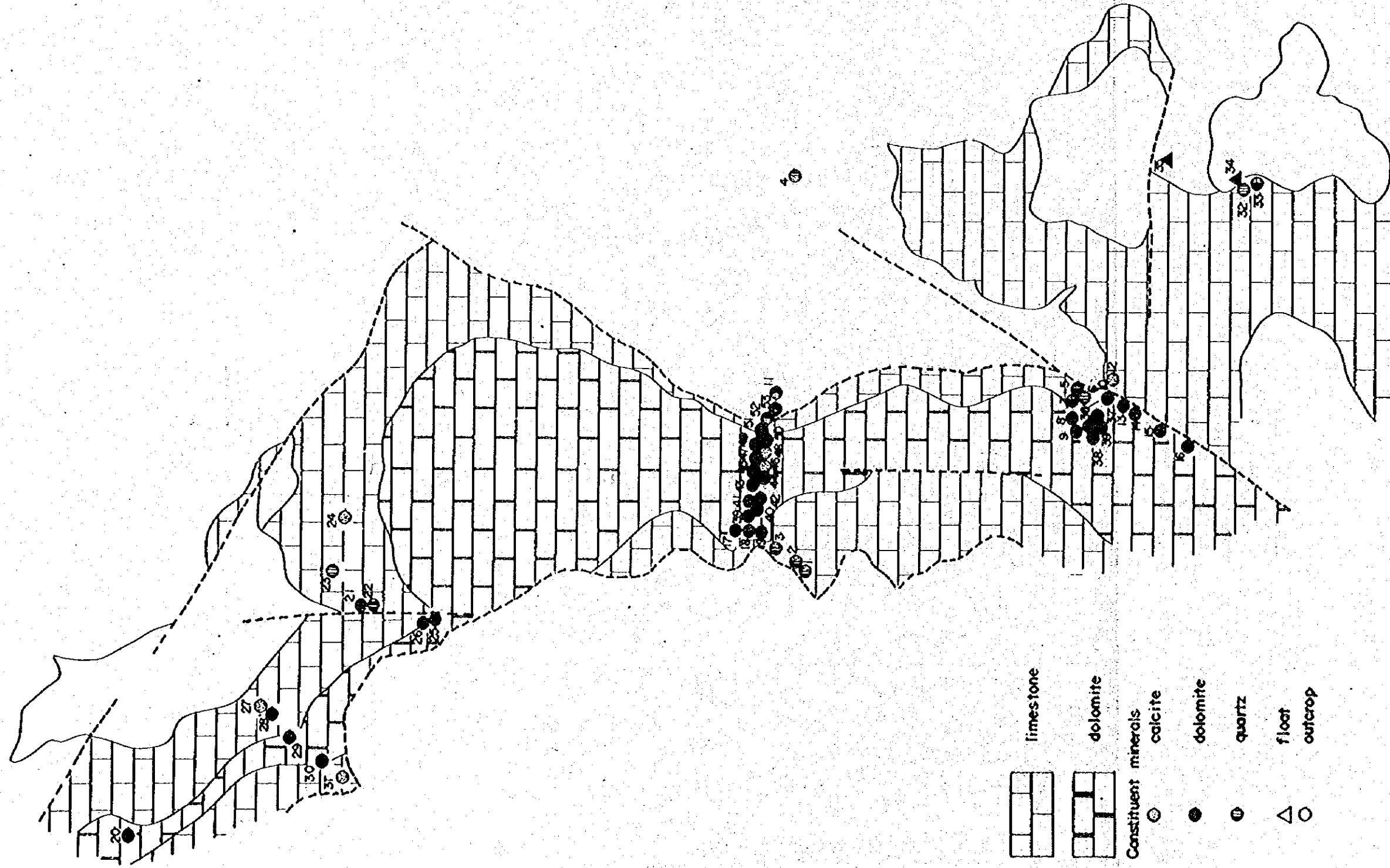
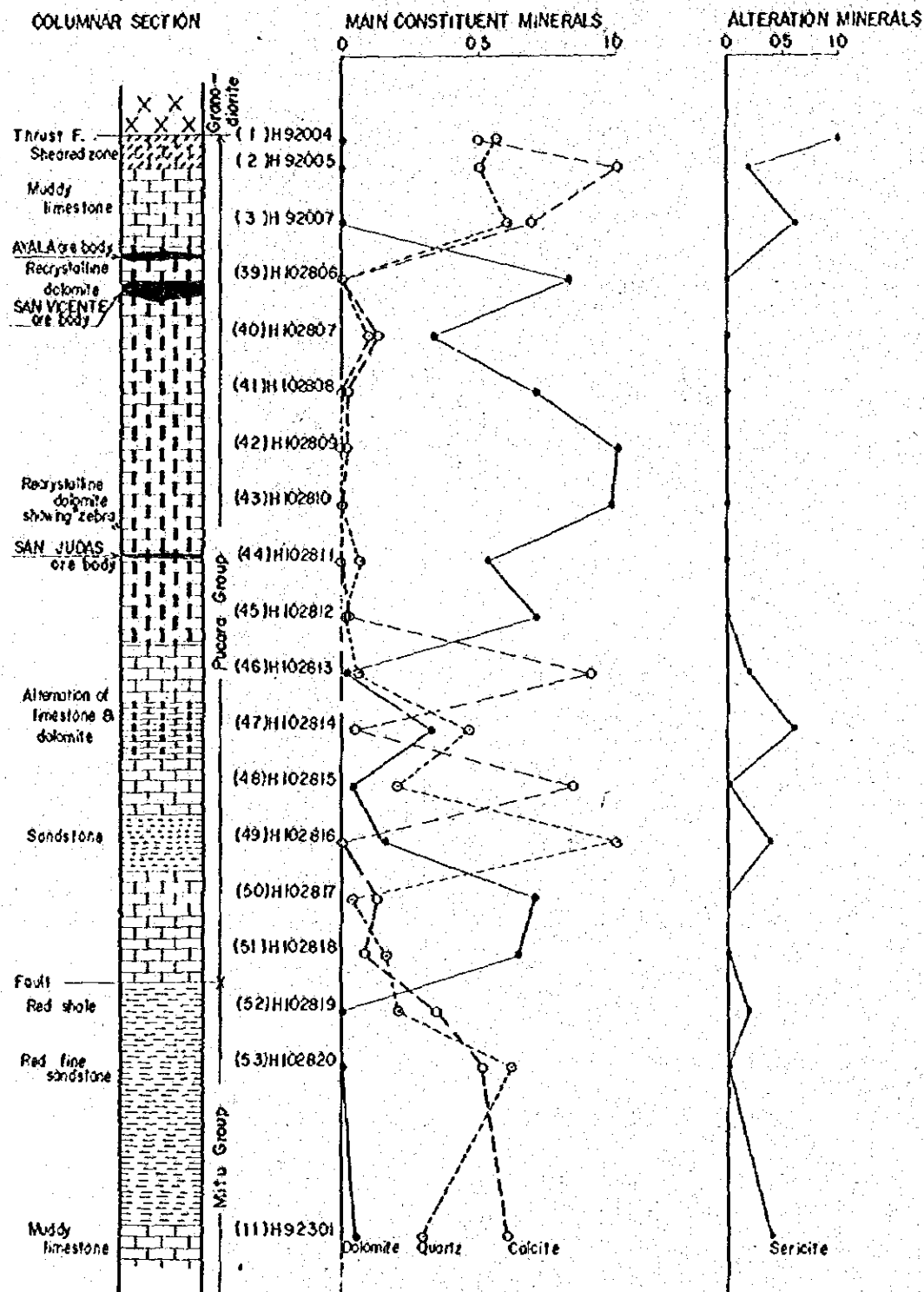


Fig. C-6 Analytical Map of the Carbonaceous Rocks by X-ray Diffraction



X Every points show the ratio of the length to the length in all samples of strongest peak about every mineral

Fig. C-7 Comparative Diagrams between the X-ray Data and Geology along the Mine Road, San Vicente

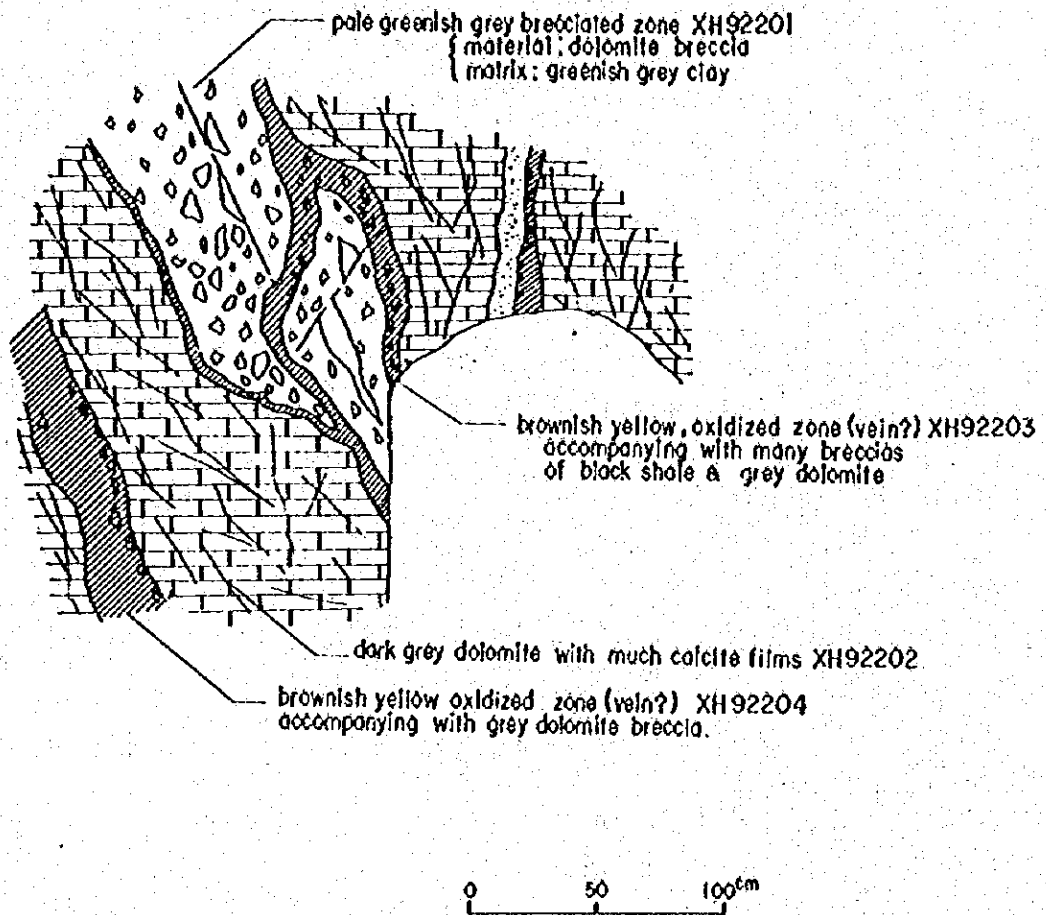


Fig. C-8 Partial Sketch of the Vein near the Siete Jeringas Ore Body

were kept constant, so that the contents of similar mineral species could be compared each other in terms of the samples. As the full scale values, 500 cps, 1,000 cps, 2,000 cps, and 5,000 cps. are applied to avoid scaling out.

By studying the results of examination, the contents by mineral species are shown on Table C-2.

The detected minerals were calcite, dolomite, quartz, plagioclase, serisite, kaolinite, chlorite, barite, pyrite, sphalerite, smithsonite, and galena.

The followings are the interpretative descriptions by minerals in relation to the field occurrences.

(1) Calcite. Calcite is commonly and abundantly observed. Mostly calcite occurs as the component mineral of limestone, but it appears as networks or veinlets in the field.

(2) Dolomite. Dolomite is commonly and abundantly observed. It is the main component mineral of dolomite rock, but it also occurs in veinlets or networks near the ore deposit. Whether the dolomite should be regarded as the altered rock associated with mineralization or not, is the problem to call for discussions as related to the genesis of ore deposits, but the dolomite minerals in the veinlets and networks are considered to be related to the mineralization.

(3) Quartz. Quartz is also observed universally. Quartz is the main component mineral of clastic rocks, and its amount varies according to the contents of clastic materials in the rock. The veinlets of quartz and silicified zone has never been recognized in the field. This may suggest that quartz occurs entirely as the component mineral of the rock and has no direct relation to mineralization.

(4) Plagioclase. It occurs in very small amount associated with dolomite.

(5) Sericite. It occurs commonly in association with calcite, though very minor in amount. In the calcareous rocks sericite is easily produced by weak hydrothermal reaction, which makes difficult to infer its occurrence to mineralization, only because of its existence. The known deposits are used to be in the dolomite where sericite is not recognized.

(6) Kaolinite. Seldomly it is recognized in very minor amount. Sample H 9004 in which kaolinite was detected, was obtained from a fault zone. The fault zone is considered to have been affoted by weak hydrothermal reaction but the relation to mineralization is not certain.

(7) Chlorite. It is seldomly found in very minor amount. The relation to mineralization is uncertain.

(8) Barite. It was found in very small amount from the samples near the ore deposits. It shows only one peak on the X-ray chart from which alone it is not proper to verify barite. Some other identification is needed.

(9) Pyrite. It is found in very minor amount but not considered to be related to mineralization.

(10) Sphalerite, Galena, and smithsonite. They are estimated as the main ore forming minerals.

As is clear from above, the alteration minerals are very few in kinds and very little in amount. It may be said on this account, that the alteration of the carbonate rocks associated with the bedded lead-zinc deposits does not exist or very rare, if any.

Putting aside what is the genesis of the badded lead-zinc deposits, the present X-ray diffraction has proved that the deposits are well developed where the dolomite content is higher in the dolomite formation (Table C-3 and Figs. C-6 and C-7).

5-3 Geochemical Survey

5-3-1 Purpose and Procedure

This survey was practiced to find out the more effective way of geochemical survey to be applied in the investigation of potentiality of mineral resources in Oxapampa Region, Central Peru; in other words, it was aimed to establish the most appropriate method of geochemical survey for the bedded zinc-lead deposits by taking up the area of the San Vicente Mine and its surroundings, the area of known deposits of this category, for the practice of geochemical operation.

412 geochemical samples were collected from this area. The sampled density was so managed that 4 samples would be taken for one square kilometer averagely, and the sampled materials were stream sediments as well as soils. Among the total of 412 samples, 173 were taken from stream sediments and the rest 239 were from soils.

The stream sediments were collected wherever the route of the precise geological survey crossed the streams, while the soil samples were collected at every 500 to 1,000 meters distance on the route.

It was made a rule to collect the stream sediments from the enriched parts of fine sands near the stream bottom. Each of the collected sample was screened by 80 mesh sieve at the spot and about 100 grams of its undersize was reserved. This was further reduced by quarterings to prepare the assay sample of about 10 grams. The soil samples were collected about 1 kilogram from the B₁-bed beneath the humus. Each sample was air dried and screened by 80 mesh sieve. About 100 grams of the undersize was taken in the field and it was later reduced into an assay sample of about 10 grams by repeated quarterings.

5-3-2 Selection of Assay Elements

Among the entire samples collected from the area of precise survey, 40 samples, approximately 10 % of all, were subjected for the multielement chemical analysis, in which 24 were taken from the stream sediments and 16 from soils. The purpose of it was to determine the most effective indicatry elements in the geochemical analysis of all the samples collected not only from the area of precise survey but also from the whole targetted area of the present survey.

The said 40 samples were examined on eight elements of Cu, Pb, Zn, Ni, As, Mo, Hg, and Mn. The results of chemical and statistical analyses are as shown on Table C-5 and C-6 . The factor analysis was made by computer on the assay values of all, excluding one soil sample (No. c-58) which was considered rejectable on account of the possible artificial pollution.

(Figs. C-10 and C-11).

Stream sediments (24 samples)	Factor 1	Zn	Pb	Figures in () show the correlation coefficients.			
		(97)	(96)				
	Factor 2	Mn	Ni				
		(86)	(83)				
	Factor 3	Cu	As				
		(66)	(66)				
Soil samples (15 samples)	Factor 1	Ni	Mo	Zn	Pb	Mn	As
		(95)	(85)	(75)	(68)	(66)	(65)
	Factor 2	Cu	Hg				
		(89)	(87)				

Followings are the comments obtained through the study of data above mentioned.

(1) As for the indicatory elements, their assay values are desirable in general to be higher in concentration and greater in deviation values.

Table C-6 Statistical Analysis of 8 Elements in Selected Geochemical Samples

() is a number of treated samples.

Stream Sediment (24)

	Cu ppm	Pb ppm	Zn ppm	Ni ppm	As ppm	Mo ppm	Hg ppb	Mn ppm
Maximum	161.0	354	8,506	697	6.1	0	97	10,842
Minimum	35	0	227	148	0.0	0	15	789
Average	23.1	35	1,245	265	1.4	0	18	4696
Standard deviation	34.6	74	2,050	110	1.9	0	17	219.1
Numbers	24	21	24	24	11	0	1	24

Soil (15)

	Cu ppm	Pb ppm	Zn ppm	Ni ppm	As ppm	Mo ppm	Hg ppb	Mn ppm
Maximum	762	89	4,969	623	14.4	5	365	2,1842
Minimum	29	0	17.8	149	0.0	0	15	1053
Average	153	29	1,353	303	3.1	0	87	5608
Standard deviation	184	27	1,641	119	4.6	1	116	557.7
Numbers	15	10	15	15	10	1	7	15

In this connection, As, Mo, and Hg are considered inadequate as the indicator, as many assay values showed below the limit of identification as 18 among 40 samples in As, 39 among 40 in Mo, and 32 among 40 in Hg.

(2) The existence of such ore zones as given below in the surveyed area has to be kept in mind.

1. In the western highland; Ni-Co ore zone in the pre-Paleozoic metamorphic rocks.
2. In the central part; Zn-Pb ore zone in the Mesozoic limestone.
3. In the central part; copper indications in the surroundings of the later intrusives.

(3) In view of the results of factor analysis, it may not be adequate to select any two elements as indicator elements from an element group variable by the same factors.

(4) The multi-genetical element such as Mn is not appropriate to be taken as an indicator element in the regional survey, as its genetical origin is hard to be identified in the data analysis.

Base upon such studies, Cu, Zn, and Ni were taken as the adequate indicator elements for the area of reconnaissance survey, while for the area of precise survey, of which targets are the zinc-lead ore zones, Cu, Zn, and Pb were chosen as the proper indicators, as Pb shows greater deviation and considered directly reflectable in the mineral exploration.

The flow-sheet of analysis of the eight elements are shown on Table C-4.

5-3-3 Results of Geochemical Survey

Various elements are contained in minor amount in the rocks quite indifferent from mineralization, but the amounts varies according to the kinds of rocks and in some specified rocks often the contents show so high values that they prevent to extract the mineralization zone.

The assayed values of each element were correlated to geology where the samples were collected in the area. This correlation was mainly done on the soil samples, as the stream sediments don't reflect geology of the spots honestly. The results tell that Cu is high in the dioritic rocks (\bar{x} : 34.9 ppm in overall samples, 59.9 ppm in dioritic rocks) and the standard deviation is bigger (46.6 ppm in overall samples, 69.4 ppm in dioritic rocks). Zn shows the higher background in the Pucara Group (\bar{x} : 142.5 in overall samples, 21.5 ppm in the Pucara Group) and the standard deviation is also bigger. (255.4 ppm in overall samples, 377.9 ppm in the Pucara Group). Thus, it is desirable that each population will be treated according to each geological unit. In view of not extremely bigger differences from the over all values, however, the entire values were treated as in one single population in this report. The results of statistical analysis of the stream sediments in Cu, Zn, and Pb are shown on Table C-8.

Extraction of the geochemical anomalies followed the divisions as mentioned below in which the figures in () show the accepted values.

Threshold values	Cu ppm	Zn ppm	Pb ppm
Transitional Zone (\bar{x})	25.1 (30)	87.0 (100)	46.7 (50)
Weak anomaly ($\bar{x} + \sigma$)	63.0 (60)	287.7 (300)	205.8 (200)
Strong anomaly ($\bar{x} + 2\sigma$)	101.0 (100)	488.3 (500)	364.9 (400)

Results of factor analysis by computer on the assays of stream sediments are as follows, in which the figures in () show the correlation coefficients.

		Zn	Pb	Cu
Factor	1	(97.9)	(97.9)	(2.0)
		Cu	Zn	Pb
Factor	2	(100.0)	(3.6)	(0.3)

From the above factor analysis, it may be interpreted that Zn and Pb have been derived from the same factor, but Cu has been from different factor from them.

The results of statistical analysis of the soil samples in Cu, Zn, and Pb are shown on Table C-8.

The geochemical anomalies were extracted according to the following divisions in which the figures in () show the accepted values.

Extraction of the geochemical anomalies followed the divisions as mentioned below in which the figures in () show the accepted values.

Threshold values	Cu ppm	Zn ppm	Pb ppm
Transitional zone (\bar{x})	34.9 (40)	142.5 (200)	64.3 (50)
Weak anomaly ($\bar{x} + \sigma$)	81.5 (80)	397.9 (400)	206.3 (200)
Strong anomaly ($\bar{x} + 2\sigma$)	128.0 (130)	653.3 (700)	348.3 (400)

Results of factor analysis by computer on the assays of stream sediments are as follows, in which the figures in () show the correlation coefficients.

Table C-8 Statistical Analysis of 3 Elements of Geochemical Samples in the Precisely Surveyed Area . () is a number of treated samples

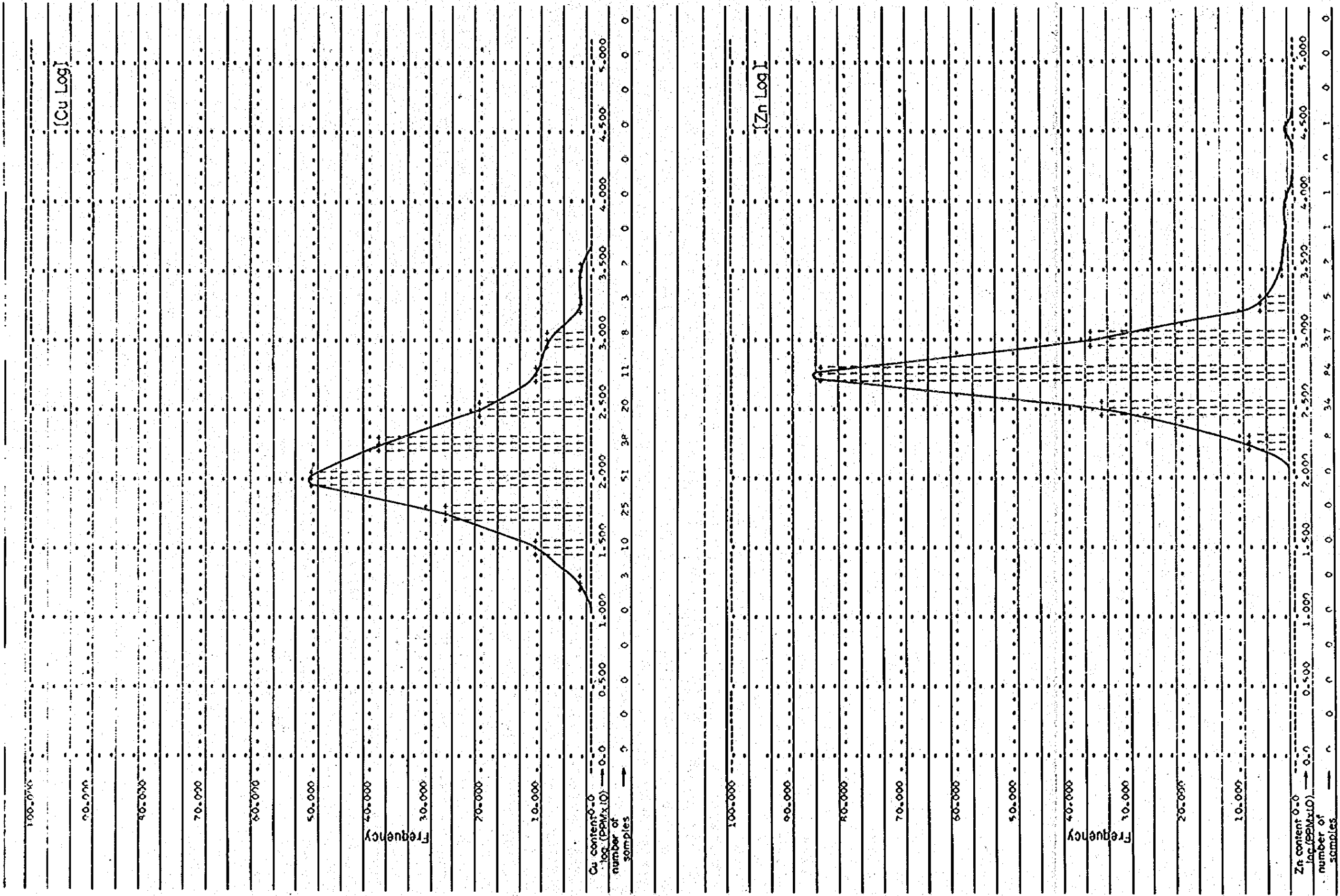
Stream Sediment [173]

	Cu ppm	Zn ppm	Pb ppm
Maximum	251.7	2,453.7	1,959
Minimum	0.0	17.4	0
Average	25.1	87.0	47
Standard deviation	37.9	200.7	159
Numbers	171	173	152

Soil [239]

	Cu ppm	Zn ppm	Pb ppm
Maximum	320.4	2,026.8	1,188
Minimum	0.0	7.2	0
Average	34.9	142.5	64
Standard deviation	46.6	255.4	142
Numbers	238	239	224

Fig. c-10 Histograms and Frequency Diagrams of Cu-Zn-Pb
(Stream Sediments)



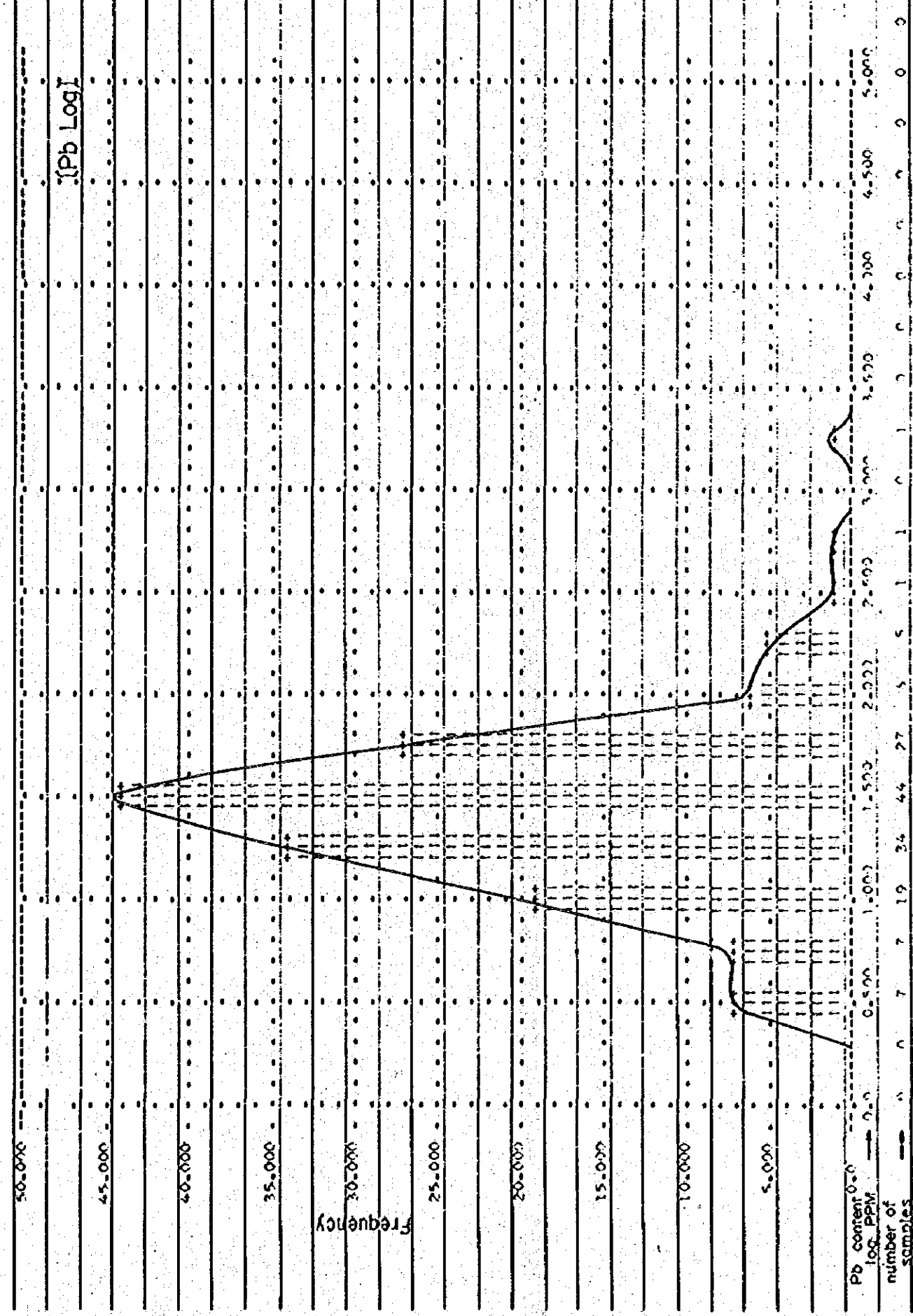
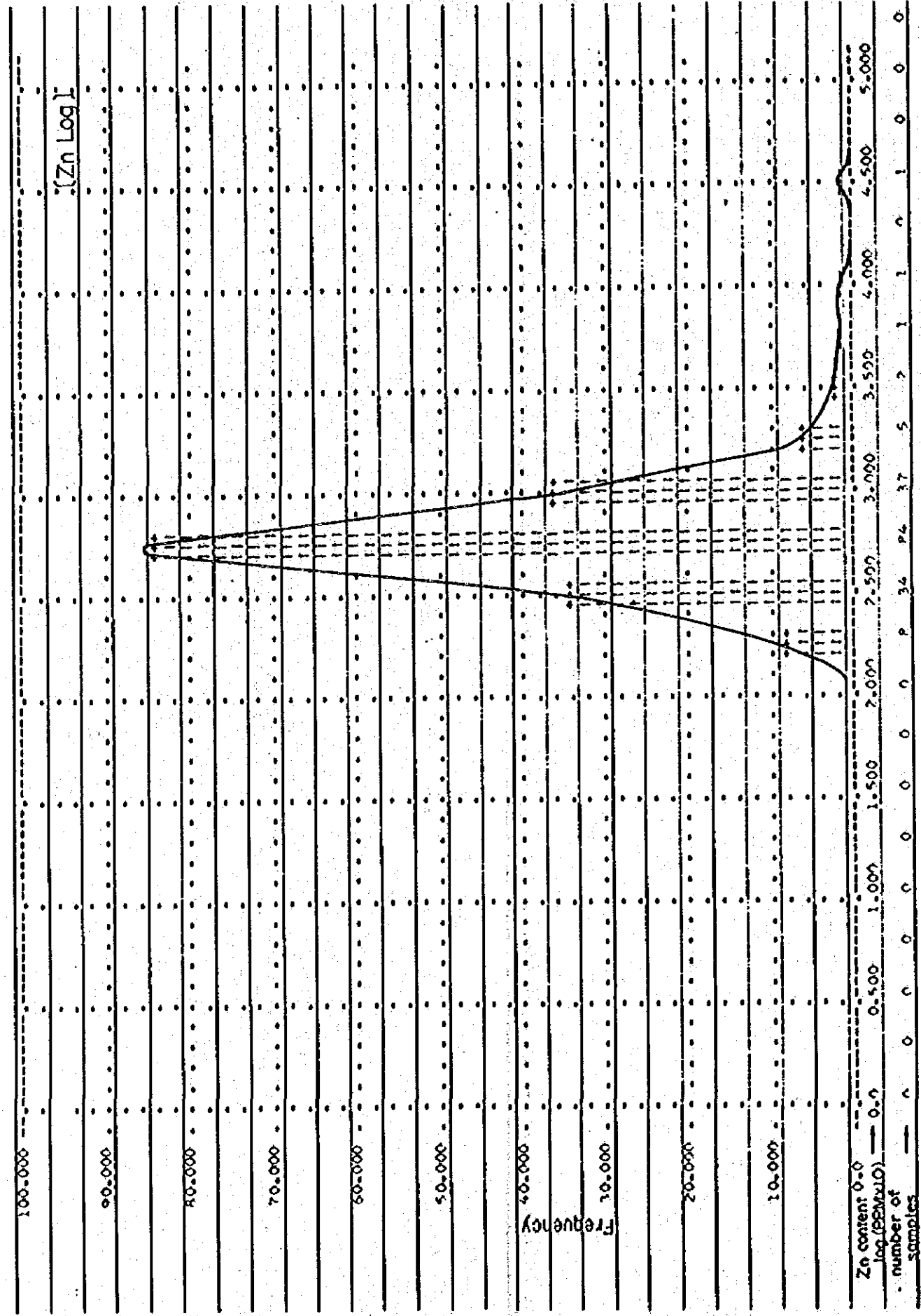
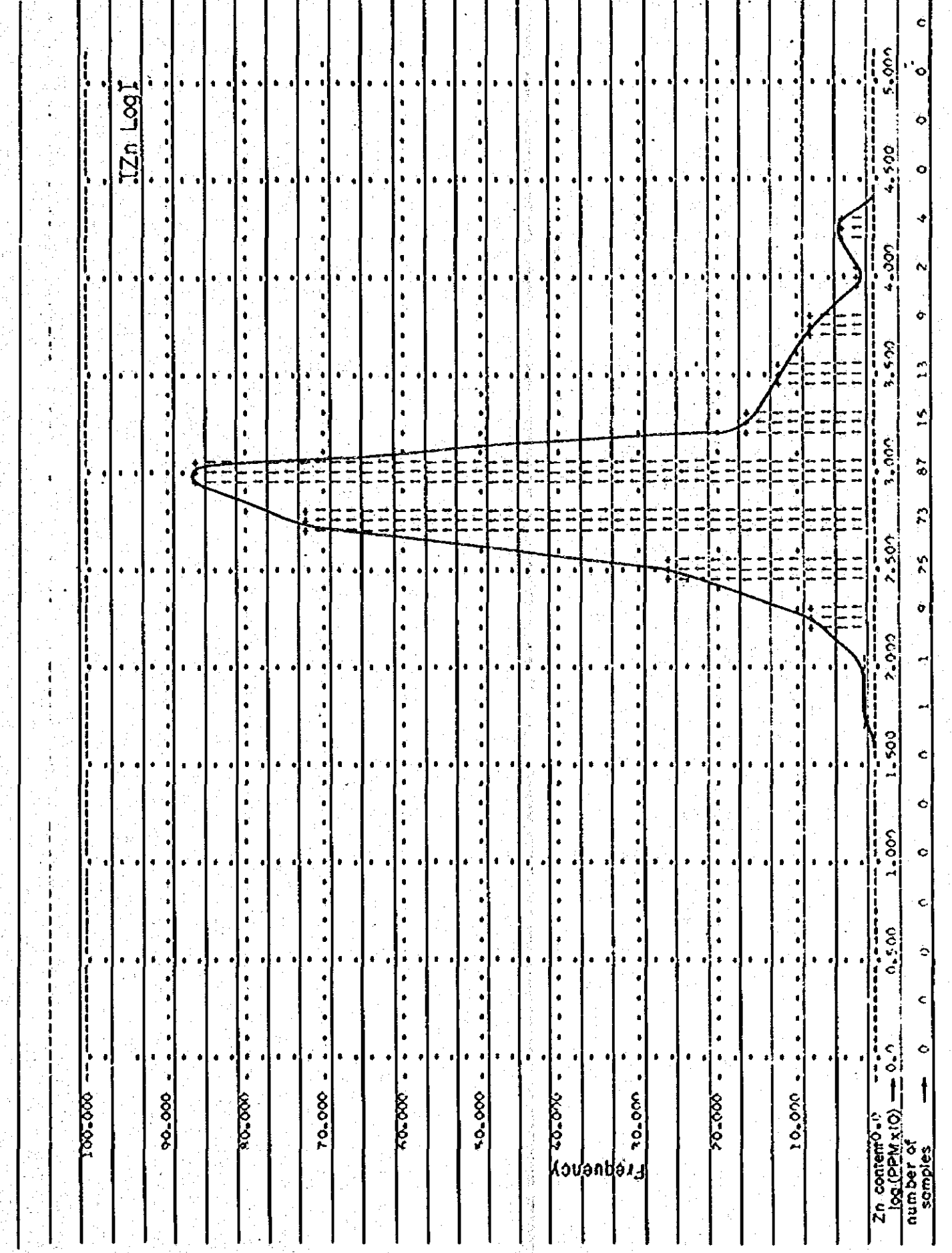
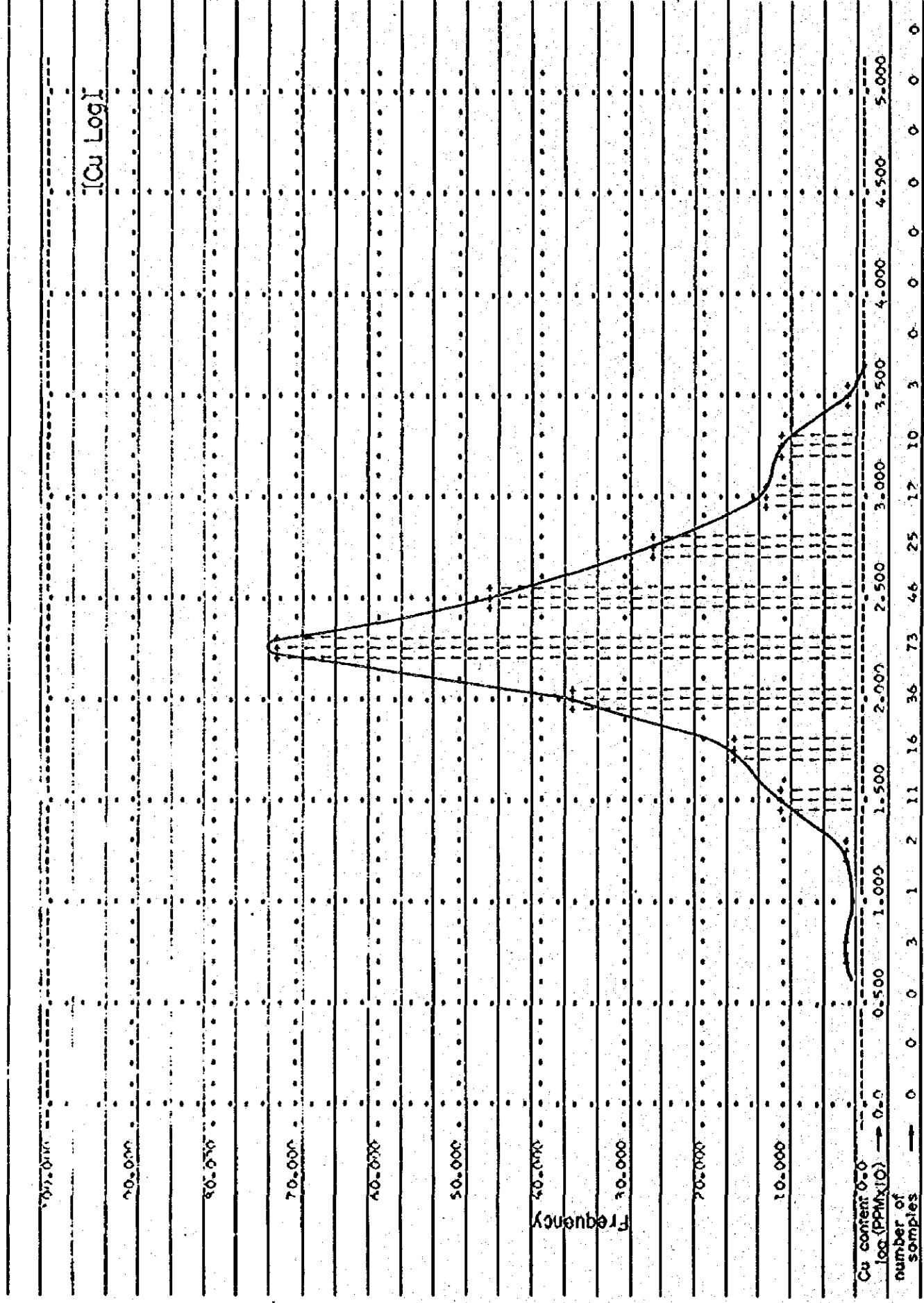
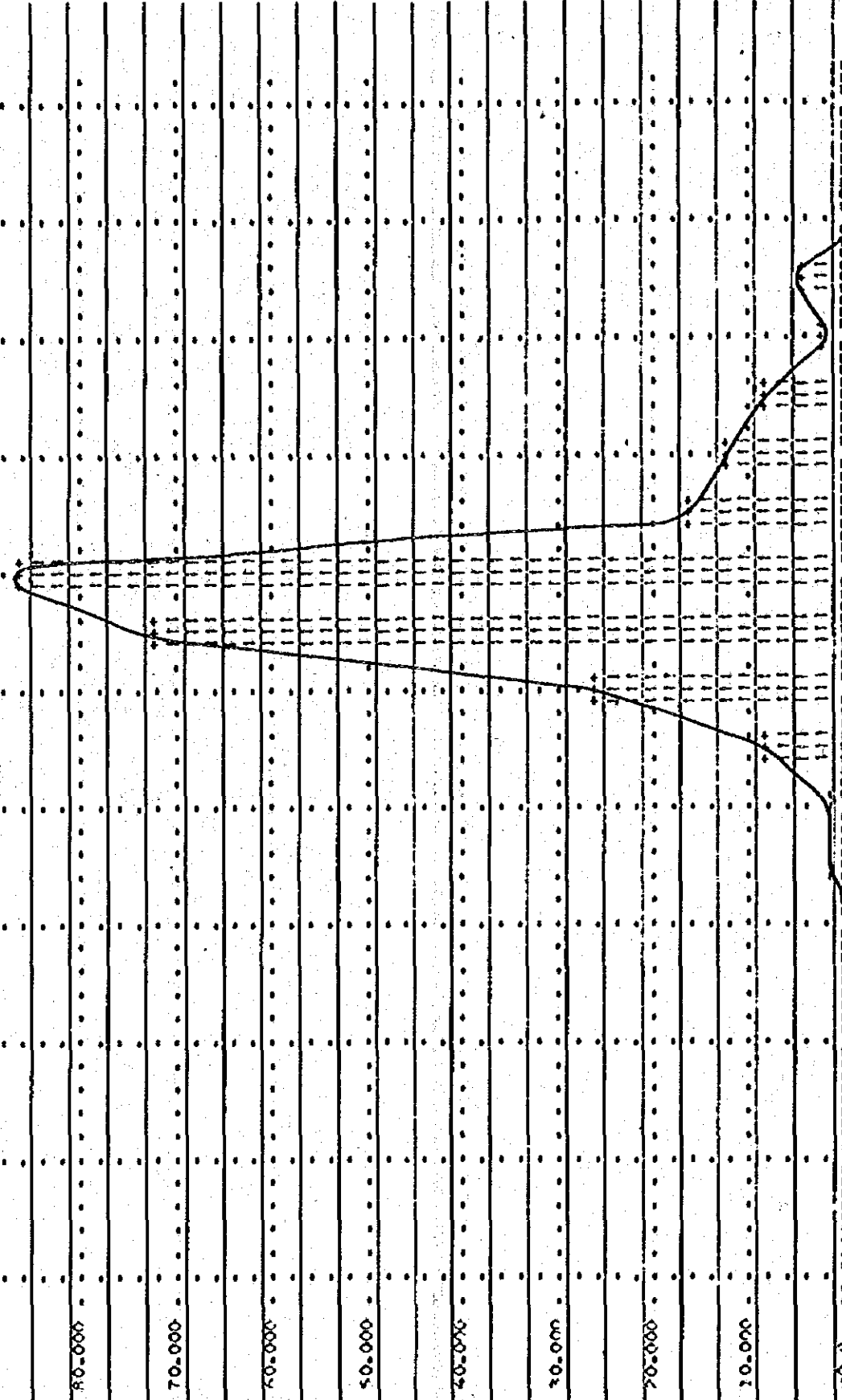


Fig. c-11 Histograms and Frequency Diagrams of Cu-Zn-Pb
(Soils)



[Zn LogI

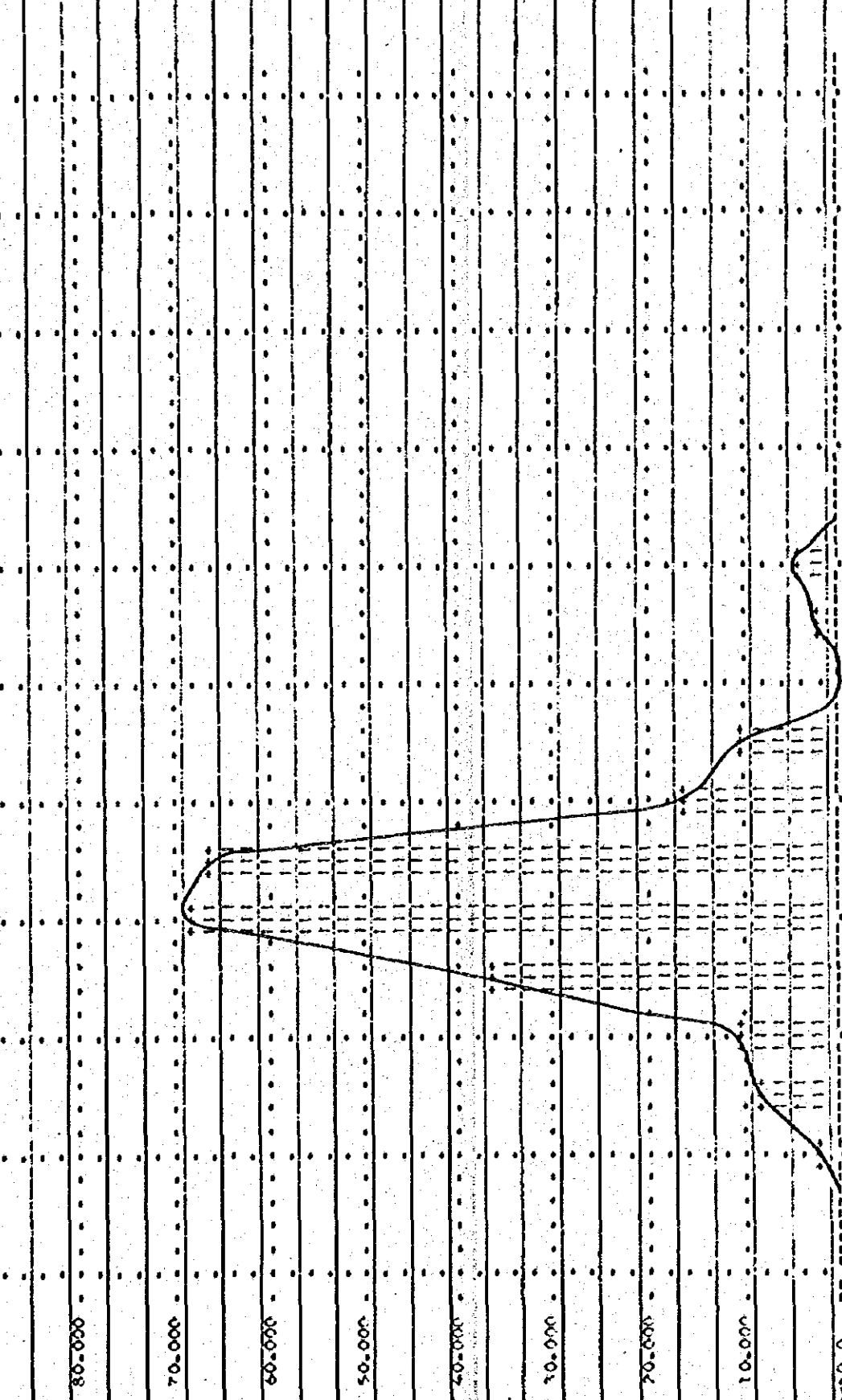
100.000
90.000
80.000
70.000
60.000
50.000
40.000
30.000
20.000
10.000



Zn content \log_{10} (PPM) $\times 10^3$ — 0.0 0.500 1.000 1.500 2.000 2.500 3.000 3.500 4.000 4.500 5.000

[Pb LogI

100.000
90.000
80.000
70.000
60.000
50.000
40.000
30.000
20.000
10.000



Pb content \log_{10} (PPM) $\times 10^3$ — 0.0 0.500 1.000 1.500 2.000 2.500 3.000 3.500 4.000 4.500 5.000

	Zn	Pb	Cu
Factor 1	(91.8)	(89.3)	(9.1)
	Cu	Pb	Zn
Factor 2	(99.3)	(17.3)	(0.5)

From the above factor analysis, it may be interpreted that Zn and Pb have been derived from the same factor, but Cu from the different factor, and possibly be related to the factor which has derived a part of Pb.

The geochemical anomalies of the stream sediments and soils are correlated in the field as follows in terms of each element.

(1) The copper anomaly by soils shows the close coincidence with the distribution of dioritic rocks, and that of stream sediments is located as derived from this igneous body. Other anomalies are all small, weak and looking unimportant.

(2) The zinc anomalies by soils are widely scattered around the known bedded lead-zinc deposits. All the areas of distribution of the Pucara Group are included in a weak anomaly. The anomaly of the down stream of Rio. Aynamayo coincides to the Quaternary sediments developed on the down stream of ore deposit zone, through which the network of trails of ore transportation are developed. This may suggest the anomaly as the overlapped pollution both natural and artificial. All other zinc anomalies by stream sediments are scattering in small ones and looking unimportant, except those derived from the known bedded lead-zinc deposits.

The lead anomalies by soils are scattered around the known ore deposits of bedded type, and the specially high anomalies are seen at the direct contact with ore deposits. A weak anomaly is also seen in the limestone nearby the northwestern dioritic rocks, from which they may possibly be related to the dioritic rocks. The Pb anomalies stream sediments are also located as

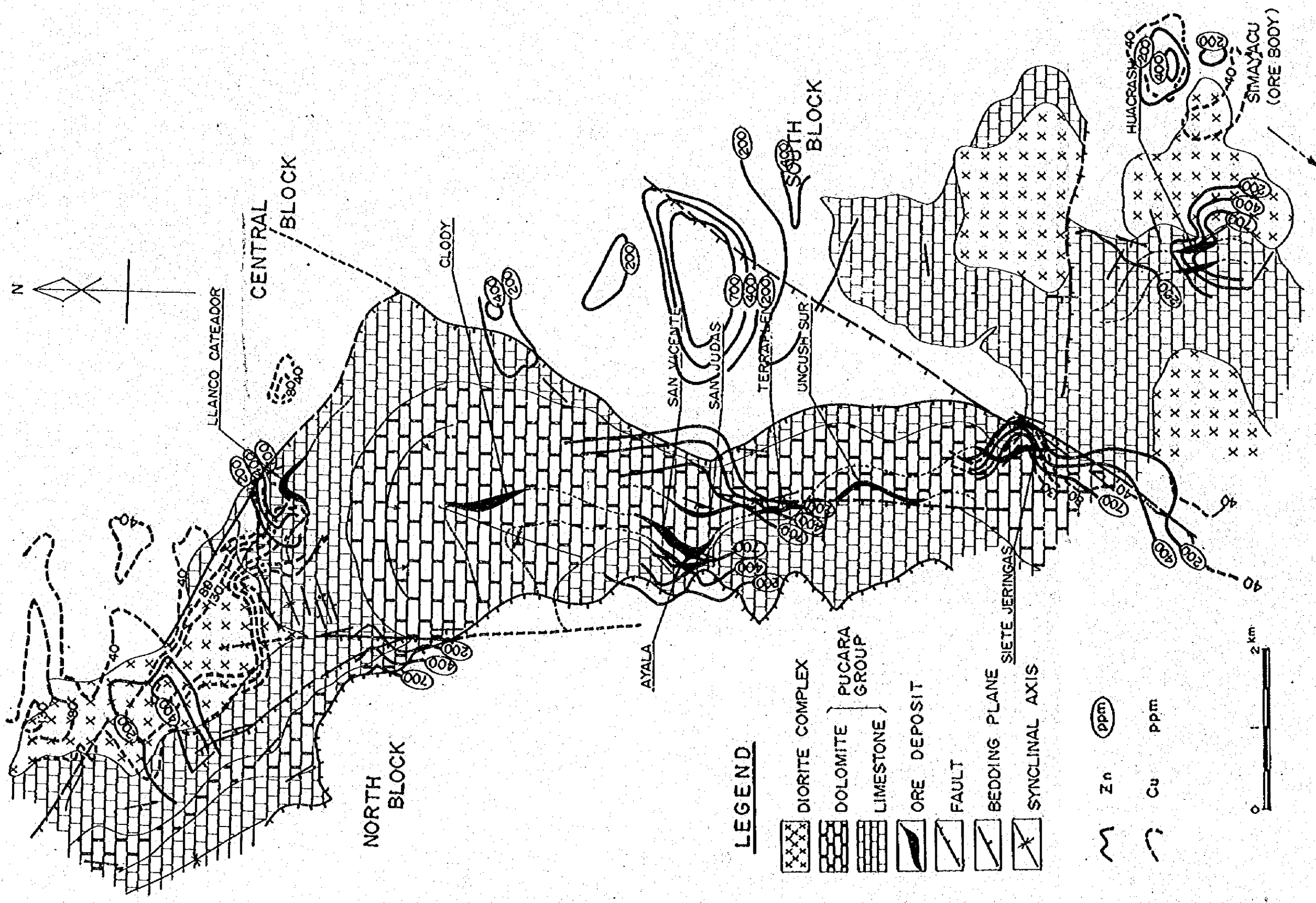


Fig. C-9. Summarized Map of the Geochemical Data of Precisely Surveyed Area (Soil Cu, Zn)

derived from the known deposits, but compared to other elements, their downward distribution is narrower. As Pb shows the shorter migration than Zn and Cu, the geochemical survey by Pb seems effective for the direct exploration of deposits in its exploration stage.

The followings are the summary of geochemical survey in the area.

(1) Geochemical survey by Zn element is very effective for the extraction of the mineralized zone of bedded lead-zinc deposits, and that of Pb is effective for the direct exploration of the deposits.

(2) Distinct Cu anomalies appear in some parts of the dioritic rocks, of which origins are interpreted as either of the following:

1) Independently from the mineralization which derived the bedded lead-zinc deposits, there took place another mineralization of mainly copper relating to the dioritic rocks.

2) Should copper be derived also from the mineralization which derived the bedded copper deposits, it might have been deposited apart from Pb and Zn.

3) The dioritic rocks are initially rich in copper themselves, and the anomaly may indicate the higher concentration of copper in them.

These facts that the alteration minerals associated with mineralization are recognized near the dioritic rocks, and that the lead-zinc deposits around them are different from the bedded lead-zinc deposits in the nature of ore, may suggest the higher possibility of the item 1). In this case the geochemical survey by Cu element is effective to extract the mineralized zone, in which the one by Pb element is desirable to be combined, as Pb may indicate the marginal zone of it (Fig. C - 9).

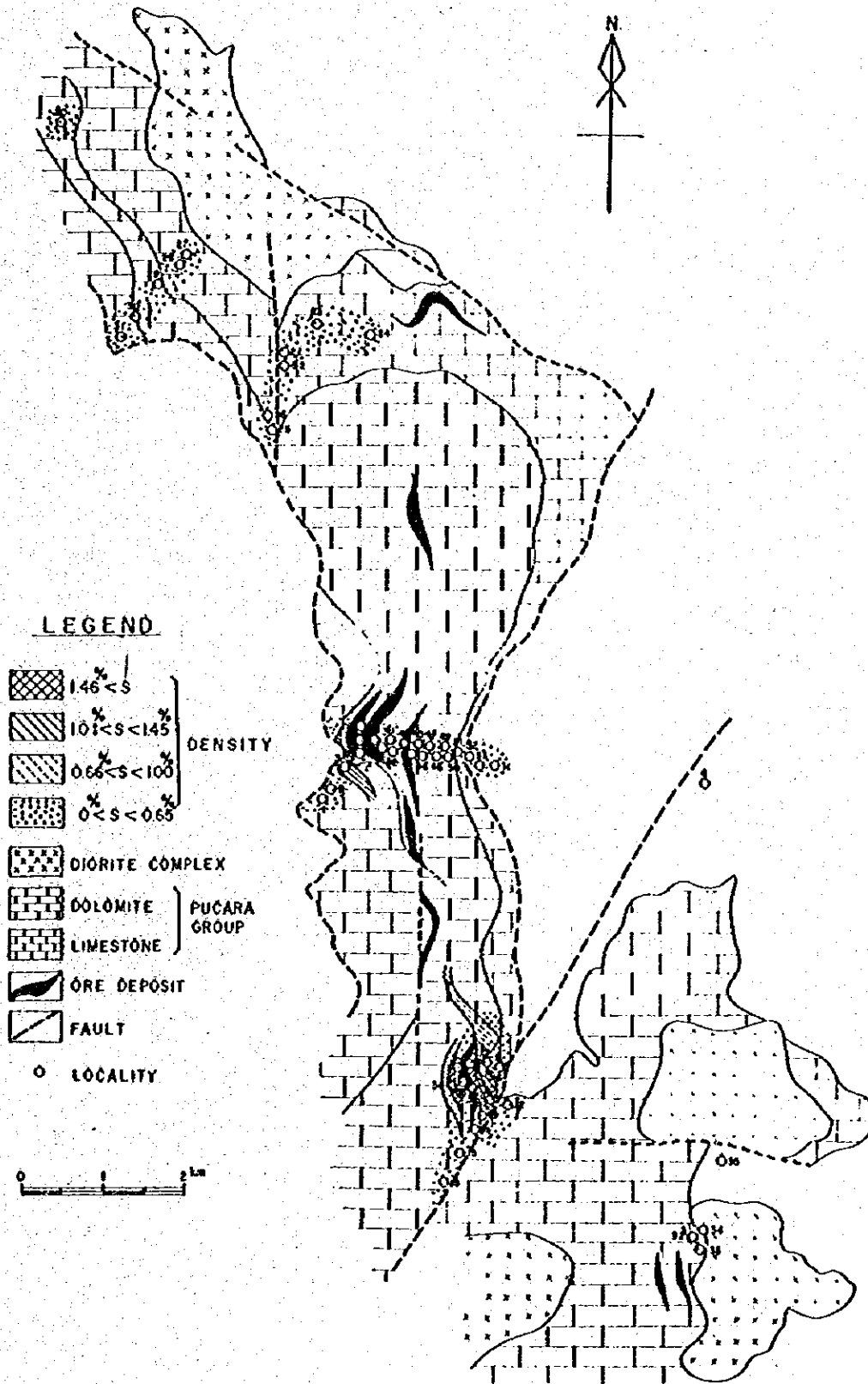


Fig.6A Contoured Map of S-Element In Carbonate Rocks

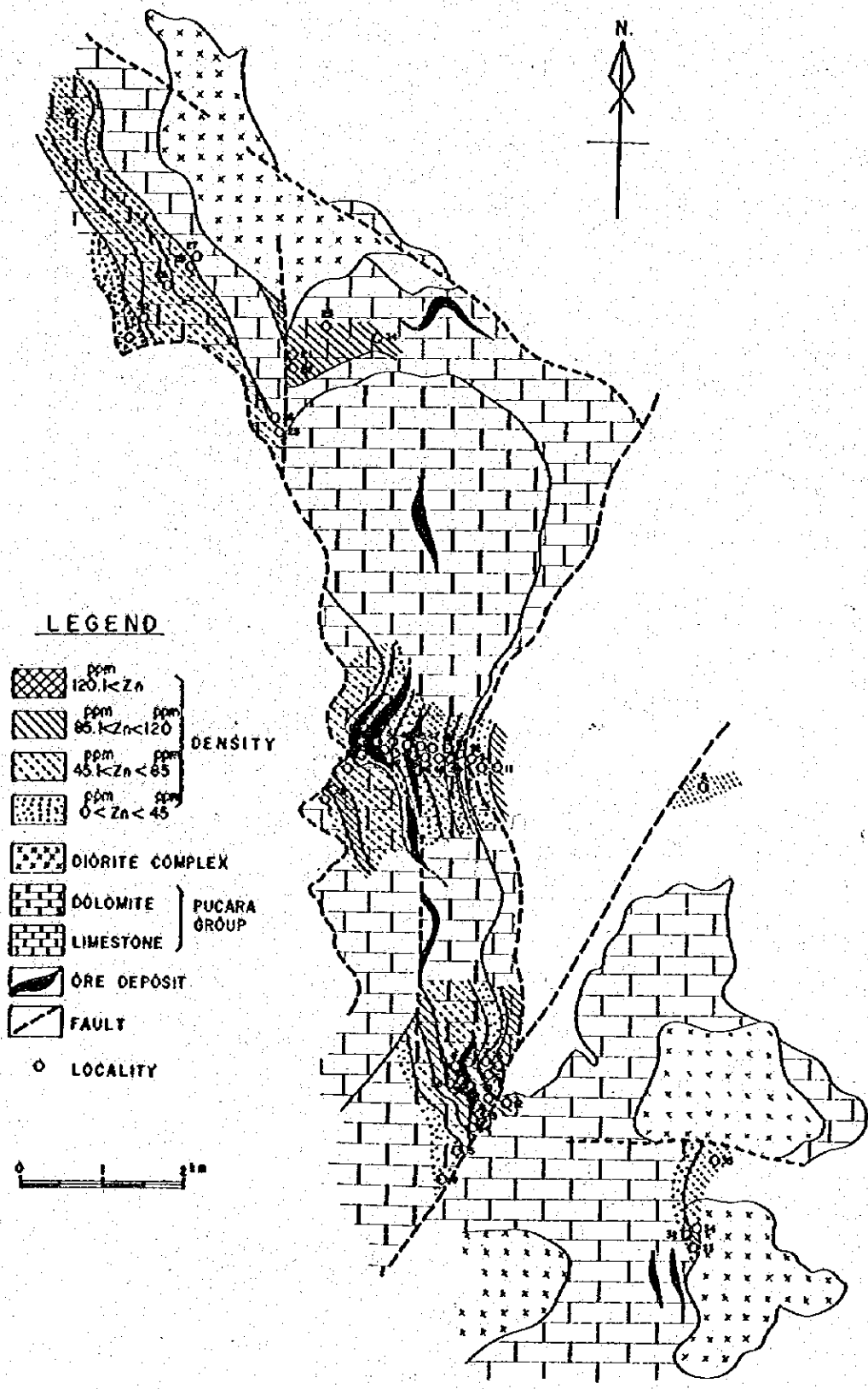


Fig.6B Contoured Map of Zn-Element in Carbonate Rocks

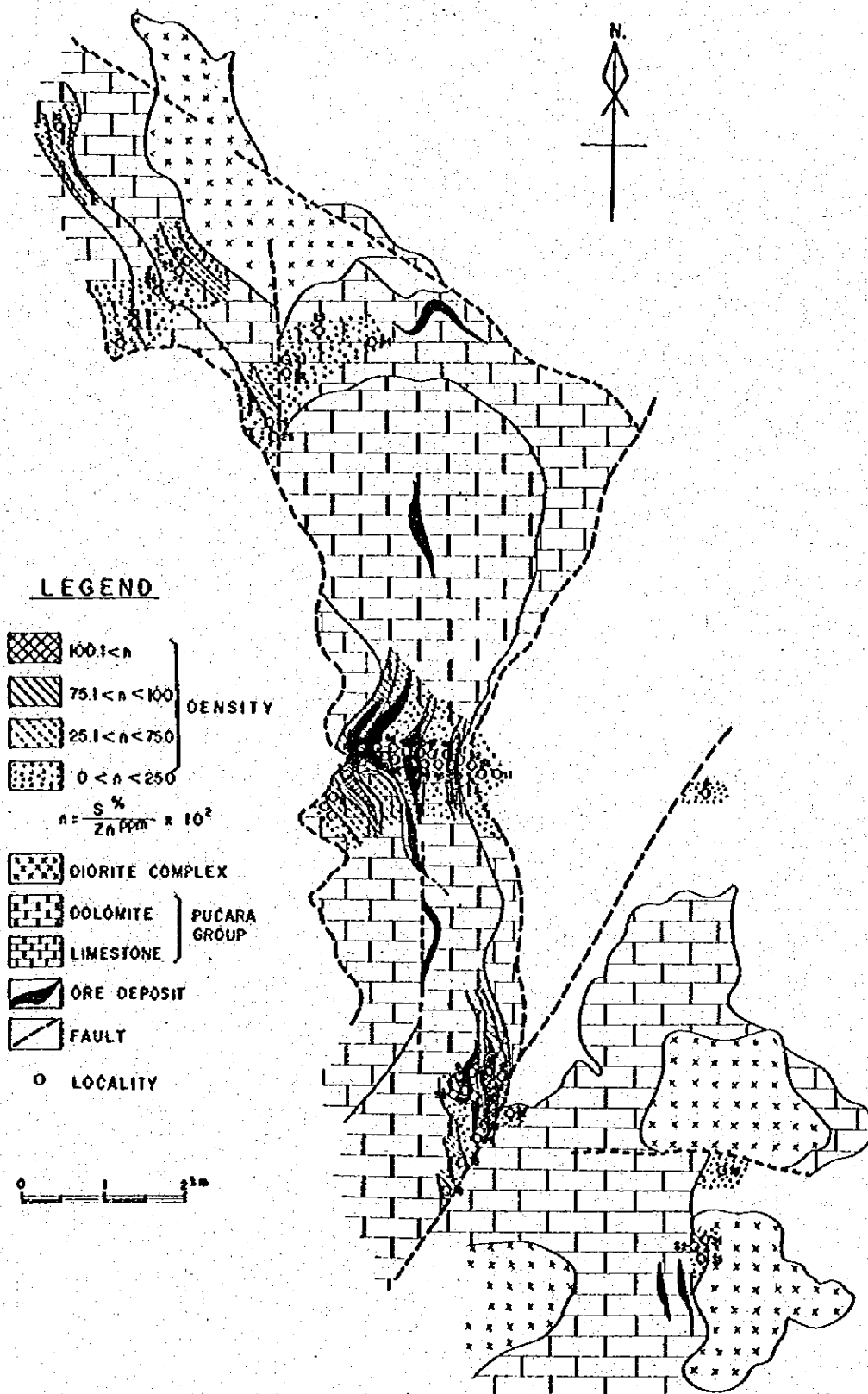


Fig.6C Contoured Map of S/Zn in Carbonate Rocks

5-3-4 Relation between Mineralization & the Minor Elements

Followings are the results of study about the relation between the mineralization and the minor elements (Zn, S) contained in the carbonate rocks near the ore deposits presently surveyed (Fig. 6, Table 17).

(1) Zn concentration in the carbonate rocks is high at Siete Jeringas and Llanco Cateador ore bodies, as well as it seems to be slightly higher in the layers of dolomite.

(2) Almost none of the difference in the concentration of S in the area, except near Siete Geringas ore body, where it is specially high.

(3) The ratio S : Zn in ppm is specially high near the known ore deposits such as San Vicente Deposits, San Judas and Siete Jeringas Deposits, and is high in the dolomite layers containing these ore deposits, too.

(4) The samples chemically analyzed are exactly same to those subjected to the X-ray diffraction, and comparison has been made on the results of the two, which says that a tendency is locally recognized higher in both Zn and S close to the San Vicente and the San Judas Deposits, but in the dolomite a little away from the deposits, lower than the outside limestone.

In view of the results stated above, such investigation of minor elements in the carbonate rocks has been found very effective method of exploration, on the way to explore the extracted mineralized zones.

5-3-5 Results of the Microscopic Examination

Followings are the results of mineral composition of ore by microscopic examination.

(a) The main ore body of San Vicente under the present operation is located nearly the center of the San Vicente Deposits, of which features are;

(1) the ore minerals are essentially sphalerite with association of very little amount of galena and chalcopyrite,

(2) exsolved fine grains of chalcopyrite are recognized in sphalerite, and they are sometimes arranged along the crystal faces of sphalerite,

(3) Fe content in sphalerite is generally not much, and 5.92 and 5.41 mol % Fe S have been obtained by X-ray diffraction, this may suggest that fairly low temperature may be anticipated in the crystallization of sphalerite,

(4) pyrite is observed in sphalerite and gangue minerals, and it may be understood to have been deposited later than the mineralization of sphalerite, judged from its occurrence.

(b) Followings are the features of ore of the Siete Jeringas Ore Body, adjacent to the dioritic stock near the southern extremity of the San Vicente Deposits;

(1) the ore minerals consist mainly of sphalerite and local concentration of galena,

(2) two stages in mineralization of sphalerite are estimated from the modes of occurrence; the first stage is simultaneous with galena and others, and the second is represented by the stringers of sphalerite traversing the sulphide minerals formed in the first stage.

(3) Fe content in sphalerite is slightly higher than the main ore body of San Vicente, showing 6.8 mol % FeS, and crystallization temperature of sphalerite is slightly higher than the main ore body of San Vicente, and

(4) fine grained pyrite is recognized, but it is inferred to have been derived from the later mineralization than sphalerite.

(c) The features of the Llanco Ceteador Ore Body near the dioritic stock

at about northern extremity of the San Vicente Deposits is almost similar to those of the Siete Jeringas Ore Body. The ore of Uncush Sur located in between the main ore body of San Vicente and the Siete Jeringas shows intermediate natures between them.

5-3-6 Examination of fluid inclusions

Followings are the results of research about the ore forming temperatures based upon the examinations of fluid inclusions in the host rocks of ore deposits and determination of their filling temperatures.

(a) Samples were collected three from the main ore body of San Vicente Deposits, one from the Siete Jeringas, and one from Uncush Sur Deposits.

(b) In the sample either of sphalerite or dolomite, most of the inclusions are so minute as less than 10 microns. The filling ratios (volume of liquid phase/volume of inclusion) are generally higher, being estimated about 95 % in measurement by eyes. It is understood from this, that the filling temperatures are fairly low. As the inclusions were so minute that few were actually determined. No determination of filling temperatures was made about the inclusions in sphalerite, as the refractive index of sphalerite was so high as the observation was made difficult. All the values were obtained through the determination of dolomite:

(c) The results of determination are shown on Table 14, from which the filling temperatures of the inclusions of dolomite are estimated within the range from 70° to 150°. Only one showed as high as 210°, but it is hard to conclude whether such high was made by leaking of the contents, or related to the dioritic stock intruded nearby. Considering from their filling ratios, the filling temperatures of the inclusions in sphalerite are anticipated not so different from those of dolomite.

(d) The temperature range above mentioned has a close resemblance to that

of the Mississippi Valley type. But the definite conclusion shall be sustained here, as the data about salt density are not available.

(e) In the deposits of the Mississippi Valley type, most of the liquid inclusions are within the range of 75° -- 130° in the filling temperatures, and 20--23 wt % in the salt densities.

As regards to the genesis of the San Vicente Deposits, no data is available to conclude definitely, but, considering from their occurrences wall rock alteration, mineral composition of ore, and the filling temperatures of fluid inclusions, the deposits are considered to have been formed under the condition of very low temperature, having a close resemblance to the lead-zinc deposits of Mississippi Valley type. However, the possibilities of diagenesis after the ore formation and migration and re-arrangement of ore materials by the Andean orogeny must not be ignored, by the reasons that the exsolved dots of chalcopyrite are recognized in sphalerite, and that the stringers of sphalerite are also recognized widely.

Considering from the ore natures, filling temperatures of fluid inclusions, and the wall rock alteration, some overlapped mineralization derived from the nearby stocks may also be possible in the deposits of Siete Jeringas and Llance Ceteador, located near the intermediate stocks intruded in the Pucara Group.

Chapter 6 Conclusion and Future Aspects

6-1 Conclusion

The present precise geological survey was carried out for the purpose to make clear how the Pucara Group are localized and distributed in the regional geological structure, as well as to establish the most effective method of exploration for the bedded zinc-lead deposits of which existence is highly anticipated in the surveyed area.

(1) Genesis of Ore Deposits

The San Vicente Ore Deposits in the center of the area are the bedded zinc-lead deposits embedded in the Pucara Group, but they were strongly affected by the diagenesis, worked upon during the accumulation of sediments, and by the intrusion of dioritic rocks. Especially, not only the dissemination of pyrite, but also the copper indications in and around the dioritic stocks accompanying the advanced alteration, may suggest that the stocks gave the compressional and thermal effects to the surrounding formations as well as they took part of mineralization. Therefore, the San Vicente deposits are considered as a peculiar type of deposits which owe their present set-up not only to the accumulation of Zn and Pb elements during the deposition of carbonate rocks, but also to the overlapping metasomatic rearrangement of elements caused by the later intrusion of the dioritic rocks.

(2) Localization of Ore Deposits

Main ore bodies in the San Vicente Mine are always embedded in the dolomite layers of the Middle part of Pucara Group and especially dominant in the banded dolomite. This dolomitization is regarded as prior to the intrusion of later igneous activity, but the process is partly represented by the veinlets traversing the sulphides. Wherever the banded dolomite is

distributed, there are developed coarse crystals of dolomite, brecciated zones, and veinlets around the formation representing the tectonical disturbed zones.

(3) Structure of Ore Deposits

Many of the faults in WNW-ESE and NNE-SSW systems formed by the lateral compression of ENE-WSW, are recognized around the San Vicente deposits, giving the ore bodies lateral dislocations. These faults of two systems are very important for the detailed exploration of the ore deposits.

6-2 Exploration Methods for Future

(1) It is important to make clear the distribution of the Pucara Group as well as to establish the zoning of dolomite layers in the Group, as the bedded Zn-Pb deposits in this area are expected to be embedded in the dolomite layers of the Group. It is necessary to establish the zoning too, as it seems possible that the ore bearing dolomite may be fixed to definite horizon.

(2) It is as well necessary to investigate the possibility of mineralization by the dioritic rocks penetrating the Pucara Group, by referring to their distribution, lithology, and structures, because they affected the Zn-Pb deposits in the Pucara Group as well as they present the dissemination of pyrite and associate copper mineralization though feeble.

(3) The Pucara Group lies over the basement complex of granitic rocks, and the inter-relation of their three dimensional structure may need to be explored either by magnetic or gravity method.

(4) The close coincidence of the distribution of the bedded Zn-Pb deposits to the Zn-Pb anomalies of geochemical survey, and that of the copper indications to the distribution of dioritic stocks and Cu anomalies of the

geochemical survey, may suggest the high applicability of the systematic geochemical survey by soils and rocks. It is desirable that any geological survey to be practiced hereafter will be carried out in combination with the geochemical survey suitable in response to the required precisity.

6-3 Future Aspects

At present moment when the fundamental survey works for the region of Central Peru have just started, it is rather difficult to propose how to carry out the future surveys. Such procedures as stated below, however, may be considered as a guide.

(1) Regional Survey

1. Structural geological survey.

Distribution and structure of the Pucara Group.

Zoning of the dolomite formation in the Pucara Group.

Distribution and structure of dioritic rocks.

2. Geochemical survey

Geochemical survey by the soils and stream sediments.

(2) Semi-regional Survey

1. Structural geological survey

Stratigraphy of the Pucara Group and detailed zoning of its dolomite formation.

Petrographical classification of dioritic rocks with reference to the related mineralization.

2. Geochemical survey

Geochemical survey by soils in and around the areas of the Pucara Group and the dioritic rocks.

Investigation of the minor elements contained in these rocks

3. Geophysical survey

Ground magnetic survey to make clear the geological structure of the Pucara Group and dioritic rocks.

(3) Local Survey

1. Structural geological survey.

Structural diamond borings,

Tracing after the specific dolomite layers and mineralization indications.

2. Geochemical survey

Grid-patterned detailed geochemical survey by soils or rocks.

3. Geophysical survey

IP survey for the patches of copper indications around the dioritic rocks.

It is desirable, therefore, the works will be carried out in order of 1. regional survey, 2. semi-regional survey, 3. local survey without the structural boring, and 4. structural boring.

APPENDICES

LIST OF APPENDICES

- Table C-3 Charts of X-ray Diffractive Analysis
- " C-4 Flow Sheets of Geochemical Analysis
- " C-5 Geochemical Data of Selected Samples on 8 Elements
- " C-7 Geochemical Data of the Precisely Surveyed Area on 3 Elements

Table C-3 Charts of X-ray Diffractive Analysis

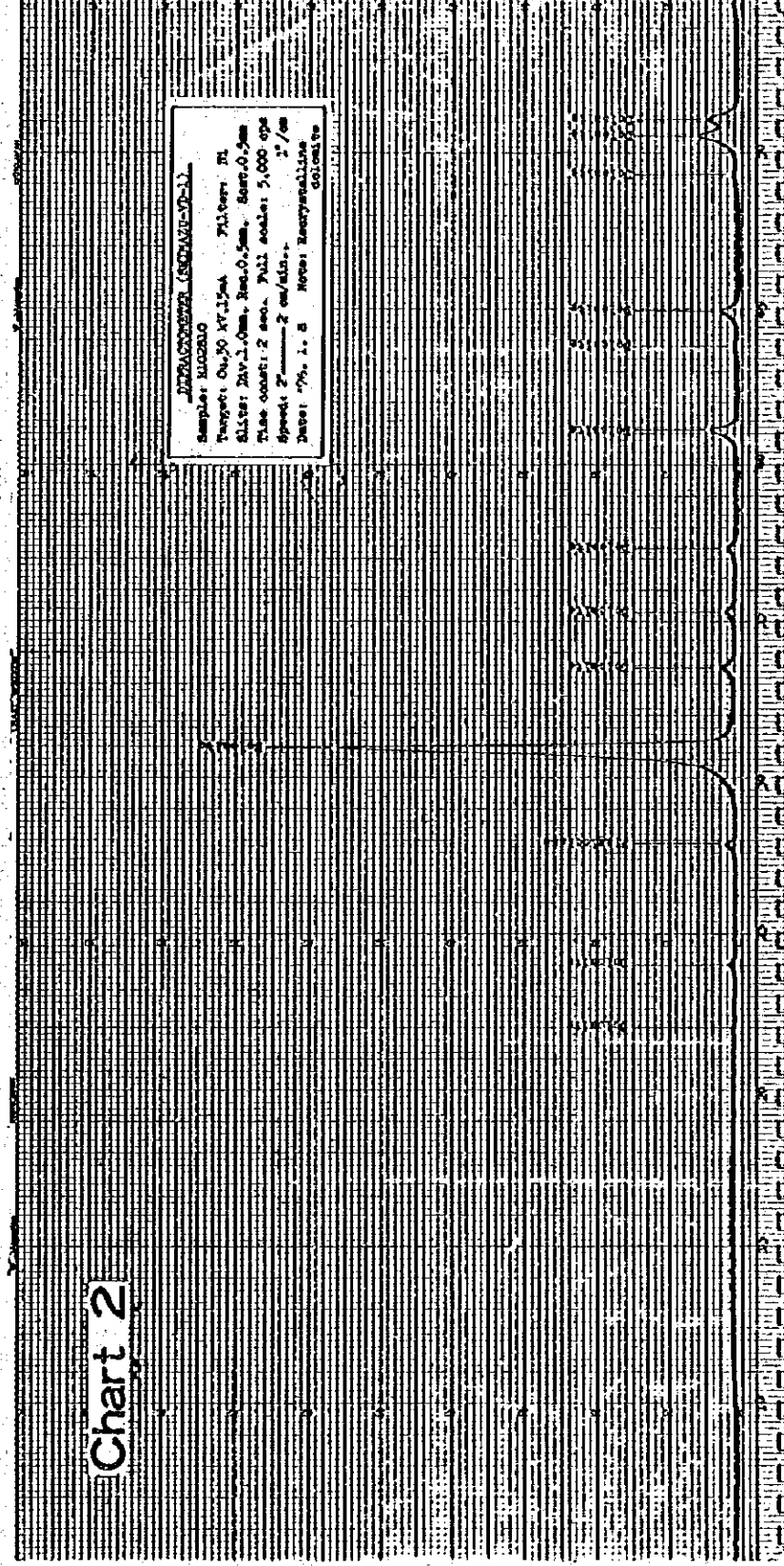
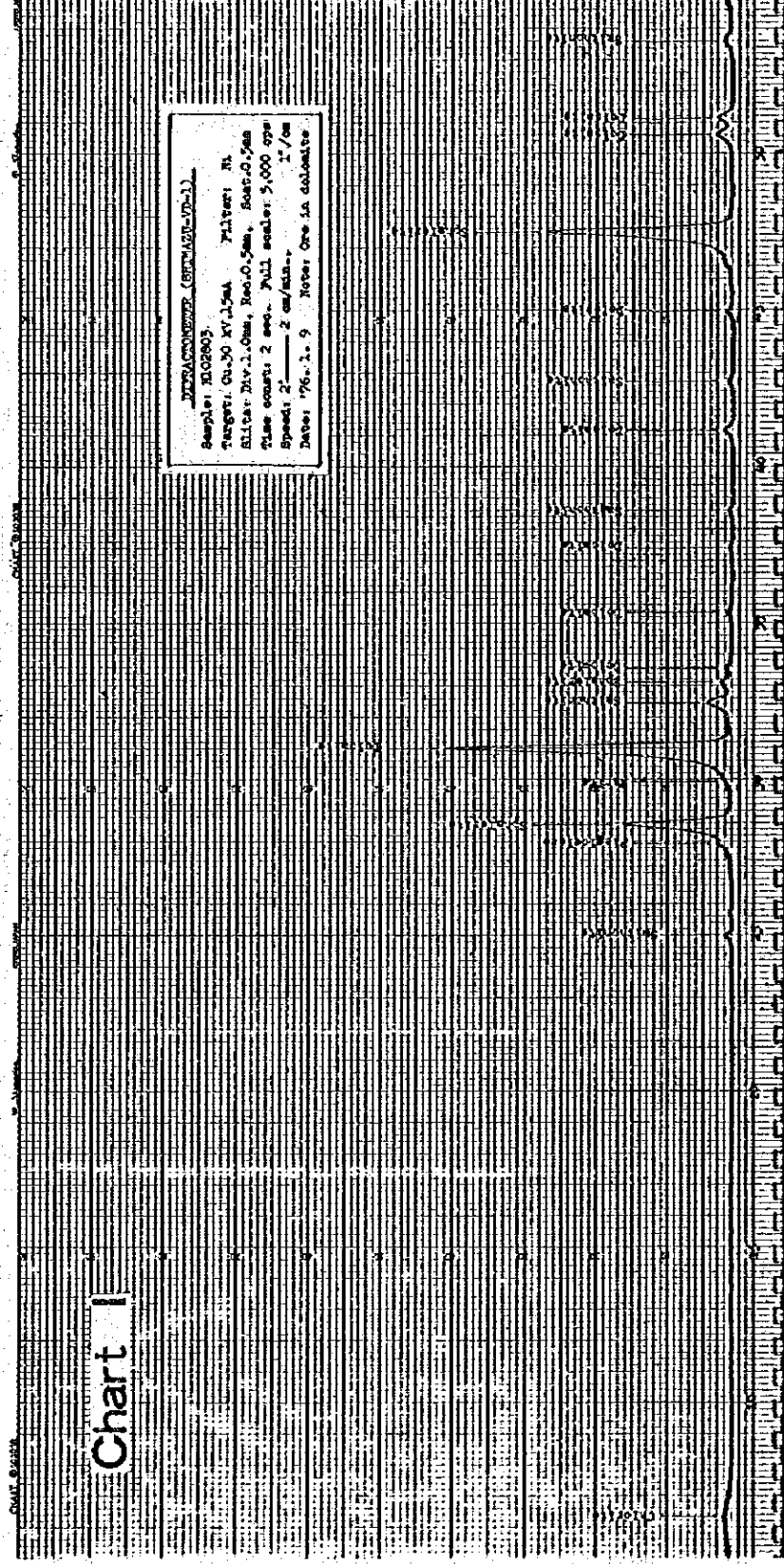
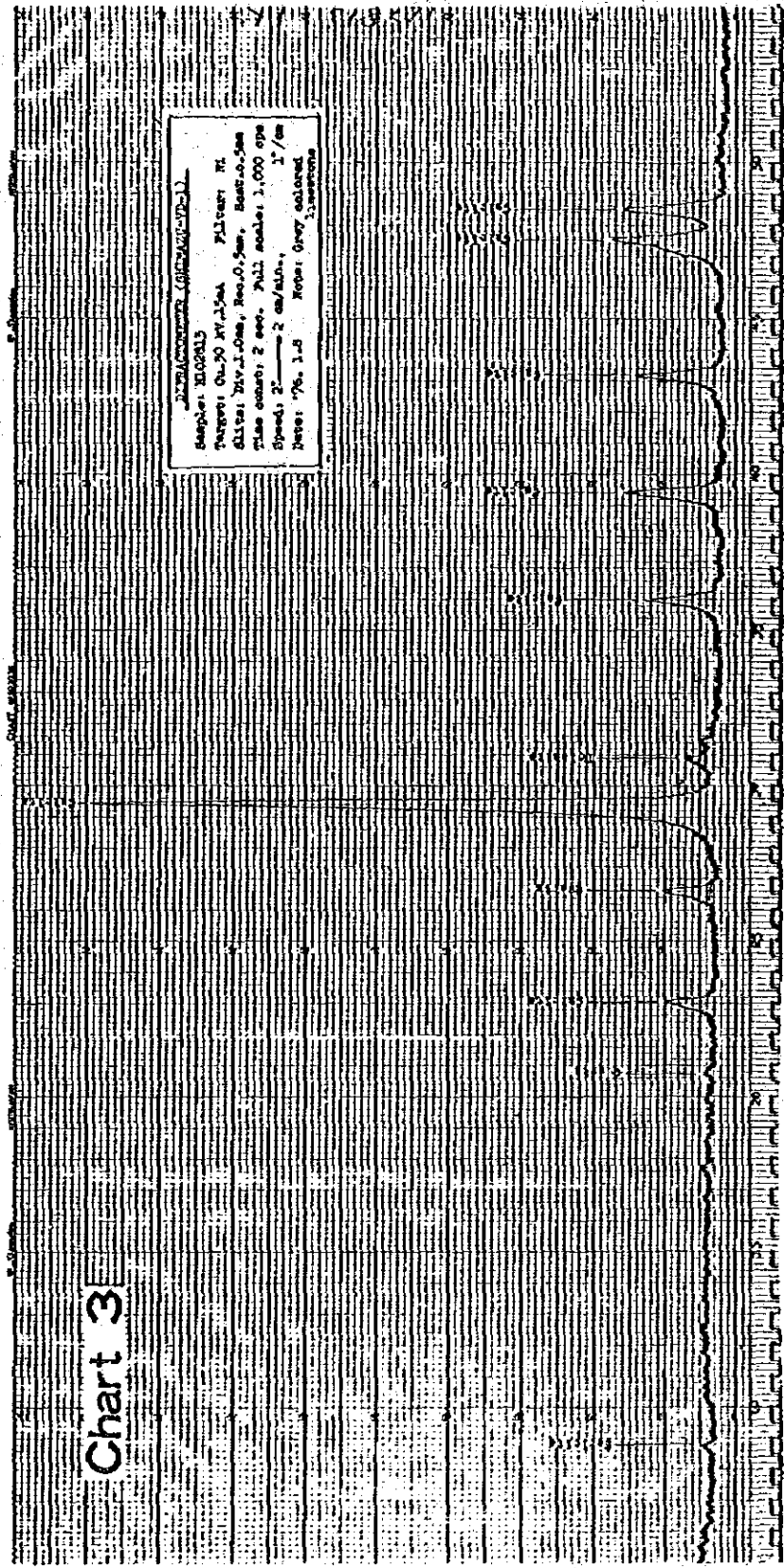
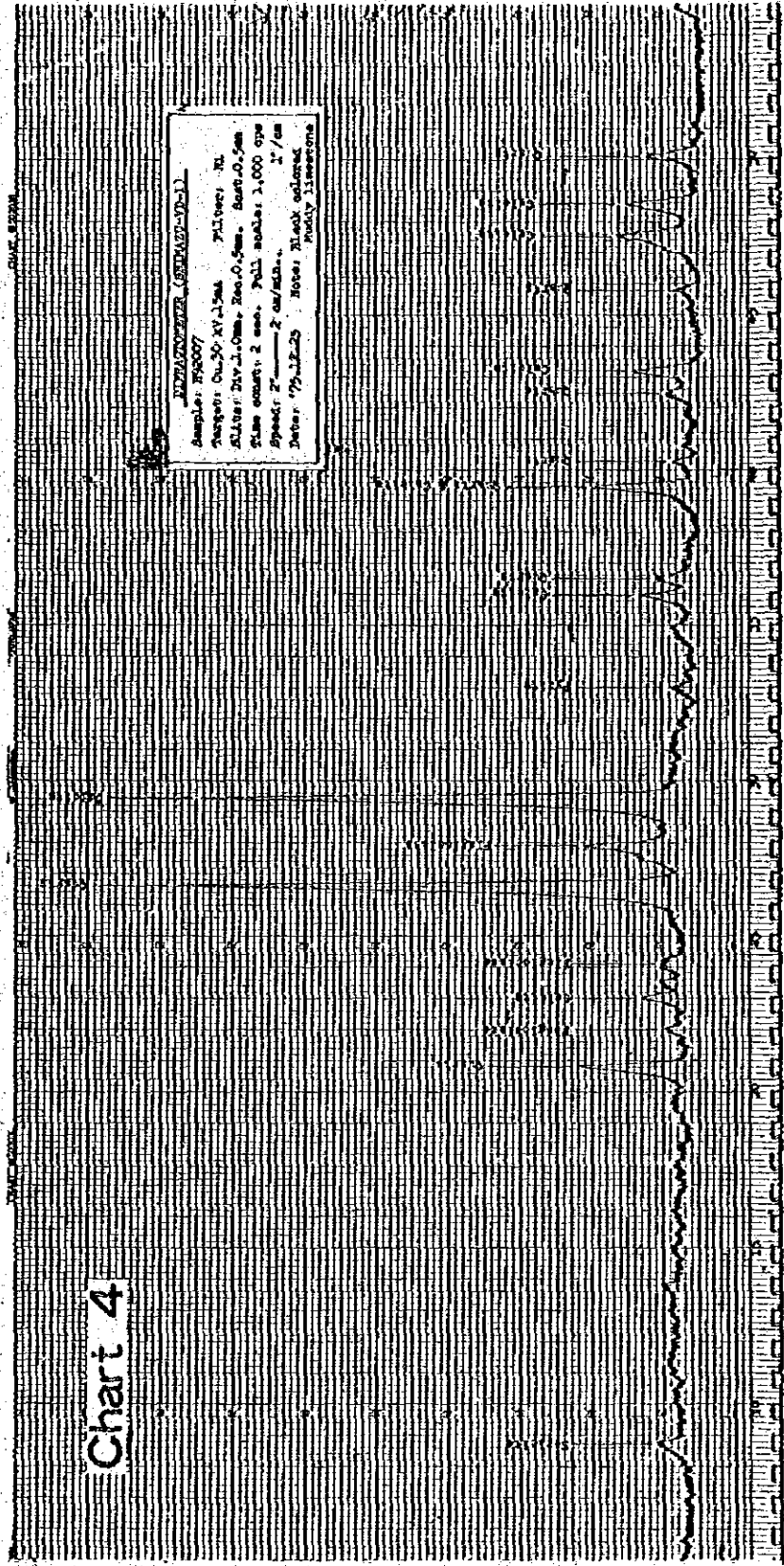


Chart 3



Sample: 810045
Target: 0u.30 4V.1.5m Filter: M
Filter: 2V.1.0m, Res: 0.5m, Band: 0.5m
Time count: 2 sec. Full scale: 1,000 cps
Speed: 2" = 2 m/sec.
Date: 7/9/53 Note: Peak colored
Study limestone

Chart 4



Sample: 810047
Target: 0u.30 4V.1.5m Filter: M
Filter: 2V.1.0m, Res: 0.5m, Band: 0.5m
Time count: 2 sec. Full scale: 1,000 cps
Speed: 2" = 2 m/sec.
Date: 7/9/53 Note: Peak colored
Study limestone

Table C-4 Flow sheets of chemical analysis

(Cu, Pb, Zn, Ni)

Sample (1 g) (in 100 ~ 300 ml conical beaker).

← HCl + HNO₃ + H₂O (3:1:1, 20 ml).

← HClO₄ (5 ml).

Evaporation for consolidation.

← (1 + 1) HCl (8 ml).

Heating for solution.

Natural cooling.

Transferring in 100 ml measuring flask.

Shaking.

Filtration (No. 6, 9 cm).

Atomic absorption.

(As)

Sample (1 g).

← $\text{HNO}_3 + \text{H}_2\text{SO}_4$ (2:1, 20 ml).

Heating for disintegration (until white smoke of sulphuric acid appears).

Cooling.

← $(1 + 1)\text{H}_2\text{SO}_4$ (10 ml).

Heating for solution.

Cooling.

Transferring to flask.

← KI (15 %, 5 ml).

$\text{SnCl}_2 \cdot 2\text{H}_2\text{O}$ (40 %, 3 ml).

Constructing the apparatus.

← Zinc grain (about 5 g).

Appearance of AsH_3 .

Colorimeter.

(Mo)

Sample (1 g).

← HCl + HNO₃ + H₂O (3:1:1, 20 ml).

← HClO₄ (5 ml).

Evaporation for consolidation.

← (1 + 1)HCl (5 ml).

Heating for solution.

Transferring to 50 ml measuring test tube.

Neutralizing by NH₄OH(1 + 1) (about 6 ml).

← Na₂CO₃ (10 %, 1 ml).

Correcting liquid measure of 40 ml.

Shaking and filtration (No. 2, 9 cm).

Dividing 20 ml into the measuring test tube.

← NH₂OH·HCl (25 ml).

← Zinc dithiol (5 ml).

Strongly shaking more than two minutes.

(showing green in colour).

Colorimeter.

(Hg)

Sample (2 g).

← $\text{HNO}_3 + \text{H}_2\text{SO}_4$ (2:1, 15 ml).

← KMnO_4 (5 %, 5 ml).

Heating for solution by water bath for two times and at $50 - 60^\circ \text{C}$.

If the color of KMnO_4 vanishes by the way, add it up to coloring.

Natural cooling.

← $\text{NH}_2\text{OH} \cdot \text{HCl}$ (30 %, a few drops up to vanishing the color).

Transferring to 100 ml measuring flask.

Shaking.

Filtration (No. 2, 11 cm).

Dividing into flask (10 - 50 ml).

Correcting up to total 105 ml.

← Reduction liquid (10 ml) (adding together 50 g of $\text{SnCl}_2 \cdot 2\text{H}_2\text{O}$ and 130 ml of (1 + 1) H_2SO_4 and adding H_2O up to total 500 ml).

Measurement.

(Mn)

Sample (1 g).

← HCl, HNO₃, H₂O (3 : 2 : 1, 20 ml).

← HClO₄ (5 ml).

Evaporation for consolidation.

← (1 + 1) HCl (8 ml).

Heating for solution.

Natural cooling.

Transferring in 100 ml measuring flask.

Shaking.

Filtration (NO. 6, 9 cm).

Atomic absorption.

Table C-5 Geochemical Data of Selected Samples on 8 Elements

Geological Index

Quaternary (gravel & sand)	(QU)
Pucara Group	(PU)
Mitu Group	(MI)
Diorite complex	(MD)
Granite & Granodiorite	(PG)

Sample No.	Stream Sediment(R) or Soil (T)	Geological Index	Content							
			Cu ppm	Pb ppm	Zn ppm	Ni ppm	As ppm	Mo ppm	Hg ppb	Mn ppm
C-21	R	PU	5.2	19	102.7	23.2	0.0	0	<30	457.9
C-26	R	PU	4.7	9	48.1	22.3	0.0	0	<30	236.8
C-30	R	QU	11.0	354	850.6	26.0	0.0	0	<30	442.1
C-31	R	QU	6.9	0	34.3	16.7	0.0	0	<30	326.3
C-42	T	PU	9.3	19	64.4	31.5	0.8	0	<30	105.3
C-53	R	MI	8.7	6	48.2	14.8	0.0	0	<30	368.4
C-54	R	MI	18.0	6	36.4	28.8	2.9	0	<30	268.4
C-57	R	MI	5.2	16	63.8	24.1	0.0	0	<30	652.6
C-58	T	MI	6.9	1188	432.9	36.2	2.9	0	<30	57.9
C-60	R	PU	5.2	0	32.7	17.6	0.0	0	<30	78.9
C-61	R	QU	9.9	0	60.1	26.0	0.0	0	<30	384.2
C-64	R	MI	7.6	0	53.0	25.1	0.0	0	<30	342.1
C-70	T	MI	2.9	0	40.1	14.9	0.0	0	<30	294.7
C-77	T	MI	9.9	0	47.4	23.2	1.9	0	<30	300.0
C-82	T	QU	76.2	62	487.8	36.2	6.3	0	335	957.9
C-132	T	MD	31.4	19	87.2	28.8	14.4	0	140	626.3
C-141	R	QU	19.7	0	53.0	28.8	0.0	0	<30	415.8
C-162	T	MI	18.6	36	87.8	39.0	1.5	0	55	447.4
C-168	T	PU	5.8	26	41.0	23.2	0.0	0	<30	121.1
C-169	T	PU	9.3	89	65.5	26.0	0.4	0	45	594.7
C-170	T	MI	12.2	33	121.8	27.8	1.2	0	145	542.0
C-177	R	MI	53.5	69	142.8	30.7	0.7	0	<30	1084.2
C-203	R	MI	13.9	33	51.4	18.6	3.8	0	<30	300.0
C-207	R	MI	10.5	9	53.4	27.8	0.0	0	<30	373.7
C-223	T	PU	3.5	43	29.8	44.6	1.9	0	100	2184.2
C-228	R	MD	161.0	23	99.8	27.8	2.6	0	<30	589.5
C-237	R	PU	4.7	49	62.8	20.4	0.0	0	97	415.8
C-242	R	PU	13.9	9	85.3	42.7	1.0	0	<30	378.9
C-245	R	PU	15.1	6	70.8	26.0	0.0	0	<30	373.7
C-265	T	PU	18.6	72	496.9	62.3	11.2	0	<30	1305.2
C-274	R	PU	4.1	46	49.9	29.7	0.0	0	<30	810.5
C-280	R	QU	12.2	6	49.8	26.0	2.6	0	<30	301.5
C-286	T	PU	9.9	19	341.5	32.5	7.5	0	<30	157.9
C-301	R	MD	3.5	0	22.7	20.4	0.0	0	<30	510.5
C-347	R	MD	83.1	125	707.3	21.3	0.5	0	<30	300.0

Sample No.	Stream Sediment(R) or Soil (T)	Geological Index	Content							
			Cu ppm	Pb ppn	Zn ppm	Ni ppm	As ppm	Mo ppm	Hg ppb	Mn ppm
C-359	R	PU	22.7	33	141.8	69.7	3.6	0	< 30	878.9
C-361	R	PU	40.7	3	47.9	29.7	5.8	0	< 30	373.7
C-388	T	MD	9.3	13	17.8	16.7	0.0	0	365	194.7
C-398	R	MD	18.0	16	75.8	19.5	6.1	0	< 30	536.8
C-412	R	MI	8.7	9	45.4	20.4	3.2	0	< 30	552.6

**Table C-7 Geochemical Data of the Precisely
Surveyed Area on 3 Elements**

Geological Index

Quaternary (gravel & sand)	(QU)
Pucara Group	(PU)
Mitu Group	(MI)
Diorite complex	(MD)
Granite & Granodiorite	(PG)

Sample No.	Stream Sediment (R) or Soil (T)	Geological Index	Cu content (ppm)	Zn Content (ppm)	Pb content (ppm)
1	R	QU	10.6	54.0	13
2	R	QU	14.2	67.6	23
3	R	QU	45.5	84.9	33
4	R	QU	13.0	49.7	36
5	T	QU	14.2	69.9	43
6	T	QU	27.8	69.4	26
7	T	QU	35.4	97.3	62
8	T	QU	13.6	67.1	39
9	T	QU	17.1	80.1	46
10	R	QU	6.5	53.2	26
11	R	QU	38.4	74.8	16
12	R	QU	8.3	50.3	26
13	R	QU	132.9	59.3	26
14	T	QU	8.9	115.4	39
15	R	QU	2.4	33.4	19
16	R	QU	23.0	74.9	39
17	T	QU	4.1	67.4	46
18	R	PG	9.4	62.3	33
19	T	PU	9.4	1,322.4	222
20	T	PG	19.5	15.1	6
21	R	PU	5.2	102.7	19
22	R	PG	11.2	50.7	23
23	T	QU	0.6	13.4	26
24	T	QU	17.7	79.7	33
25	T	QU	14.2	24.1	39
26	T	QU	4.7	48.1	9
27	T	MI	41.9	48.7	39
28	T	QU	13.0	355.2	89
29	T	QU	49.6	51.0	36
30	R	QU	11.0	850.6	354

Sample No.	Stream Sediment (R) or Soil (T)	Geological Index	Cu content (ppm)	Zn Content (ppm)	Pb content (ppm)
31	R	QU	6.9	34.3	0
32	R	QU	5.3	30.6	23
33	R	QU	4.7	51.7	69
34	R	QU	10.6	34.7	23
35	R	QU	8.3	39.9	19
36	R	MI	8.3	57.3	23
37	R	MI	4.7	34.1	29
38	R	MI	6.5	92.9	56
39	R	QU	44.9	96.7	29
40	R	QU	4.7	2,453.7	1,959
41	T	PU	14.8	97.3	56
42	T	PU	9.3	64.4	19
43	T	QU	10.0	127.6	46
44	T	QU	15.9	91.4	36
45	T	QU	9.4	2,026.8	172
46	T	QU	6.5	761.2	99
47	T	MI	226.2	24.6	59
48	R	MI	79.7	79.4	36
49	T	MI	5.9	27.2	10
50	R	MI	27.8	36.2	26
51	R	MI	13.0	46.5	19
52	R	PU	10.0	27.7	12
53	R	MI	8.7	48.2	6
54	R	MI	18.0	36.4	6
55	R	MI	4.7	71.1	39
56	R	MI	5.3	95.8	79
57	R	MI	5.2	63.8	16
58	T	MI	6.9	432.9	1,188
59	R	PU	8.9	50.7	16
60	R	MI	5.2	32.7	0

Sample No.	Stream Sediment (R) or Soil (T)	Geological Index	Cu content (ppm)	Zn Content (ppm)	Pb content (ppm)
61	R	QU	9.9	60.1	0
62	T	QU	18.3	340.3	79
63	T	MI	6.5	57.6	43
64	R	MI	7.6	53.0	0
65	T	MI	17.7	120.1	39
66	T	MI	16.5	105.6	33
67	T	MI	22.4	142.4	49
68	T	MI	46.1	435.8	49
69	T	MI	24.2	180.0	26
70	T	MI	2.9	40.1	0
71	T	MI	26.6	141.5	33
72	R	MI	3.5	77.4	46
73	R	MI	7.7	56.6	26
74	R	MI	6.5	43.5	23
75	T	PG	20.1	68.9	46
76	T	MI	20.1	88.2	43
77	T	MI	9.9	47.4	0
78	T	PG	6	82.4	39
79	T	PG	12.4	96.3	36
80	T	QU	20.7	96.5	179
81	T	QU	39.0	143.9	39
82	T	QU	76.2	487.8	62
83	T	MD	34.3	135.4	39
84	T	QU	38.9	88.2	43
85	T	QU	11.8	331.3	26
86	T	QU	27.2	112.9	46
87	T	QU	37.2	120.3	36
88	T	QU	31.9	104.8	36
89	T	QU	22.4	142.0	29
90	R	PG	12.4	119.3	16

Sample No.	Stream Sediment (R) or Soil (T)	Geological Index	Cu content (ppm)	Zn Content (ppm)	Pb content (ppm)
91	R	MI	15.4	54.5	19
92	R	MI	14.2	59.5	19
93	R	MI	12.4	51.2	23
94	R	MI	3.5	32.1	19
95	R	QU	16.5	71.1	23
96	R	QU	18.3	69.8	16
97	R	QU	14.8	63.5	16
98	R	QU	16.5	57.1	29
99	T	PU	8.9	122.1	39
100	T	PU	153.0	1,477.6	1,083
101	T	PU	26.0	310.4	235
102	T	PU	4.1	70.9	46
103	T	PU	26.0	683.6	66
104	T	PU	23.6	411.9	218
105	T	PU	49.6	458.2	185
106	T	MD	33.7	129.1	39
107	T	MD	67.3	83.9	23
108	T	MD	33.1	72.1	33
109	T	MD	44.3	138.5	76
110	R	PU	8.3	92.2	39
111	R	MD	28.9	94.2	139
112	R	MD	66.1	81.7	3
113	R	MD	63.8	90.7	13
114	R	MD	28.9	81.4	13
115	R	MD	22.4	68.8	9
116	T	QU	122.2	307.5	152
117	T	QU	41.3	111.0	23
118	T	MD	142.3	376.1	125
119	T	MD	68.5	163.3	112
120	T	QU	78.5	141.2	59

Sample No.	Stream Sediment (R) or Soil (T)	Geological Index	Cu content (ppm)	Zn Content (ppm)	Pb content (ppm)
121	T	MD	46.7	126.6	46
122	T	MI	25.4	136.0	36
123	R	MI	115.2	307.5	162
124	T	MD	75.0	164.0	66
125	T	MD	93.3	79.7	79
126	T	MD	88.6	147.0	59
127	T	MI	35.4	63.9	36
128	T	MD	13.6	72.1	26
129	T	PU	1.2	72.4	26
130	T	PU	5.9	53.3	23
131	T	MI	12.9	43.6	8
132	T	MD	31.4	87.2	19
133	T	PU	2.3	23.6	0
134	T	MI	50.3	88.5	58
135	T	QU	57.5	80.6	54
136	T	MD	18.2	26.8	8
137	T	QU	26.3	65.1	50
138	R	MD	42.1	101.8	40
139	R	QU	10.5	49.8	8
140	R	QU	18.2	44.9	4
141	R	MI	19.7	53.0	0
142	R	QU	13.8	45.6	16
143	R	MI	24.9	39.2	0
144	R	MI	12.4	33.3	0
145	R	MI	9.1	48.3	8
146	R	MI	1.4	19.1	0
147	R	MI	1.9	19.4	0
148	R	MI	4.3	37.1	0
149	R	MI	6.2	22.4	0
150	R	MI	2.8	27.2	0

Sample No.	Stream Sediment (R) or Soil (T)	Geological Index	Cu content (ppm)	Zn Content (ppm)	Pb content (ppm)
151	R	MD	9.1	45.7	16
152	T	QU	6.1	46.4	0
153	T	QU	20.0	85.0	16
154	T	QU	31.2	94.8	10
155	T	QU	22.0	77.4	6
156	T	QU	10.7	76.7	16
157	T	QU	14.8	77.4	6
158	T	QU	23.0	67.2	4
159	T	QU	32.5	83.8	20
160	T	QU	22.0	65.2	0
161	T	QU	23.0	59.8	20
162	T	MI	18.6	87.8	36
163	R	MI	100.6	303.4	172
164	T	MI	65.0	112.7	67
165	T	MI	14.8	38.5	0
166	T	MI	6.2	34.2	0
167	T	PU	11.0	120.7	33
168	T	PU	5.8	41.0	26
169	T	PU	9.3	65.5	89
170	R	QU	12.2	121.8	33
171	R	QU	8.6	38.6	4
172	R	QU	8.6	39.7	0
173	R	QU	11.9	41.7	12
174	R	QU	12.9	45.0	4
175	T	MI	10.5	43.2	0
176	R	MI	11.0	60.4	0
177	R	MI	53.5	142.8	69
178	R	MI	14.3	85.4	8
179	R	MI	11.0	39.0	4
180	T	MI	10.5	41.2	0

Sample No.	Stream Sediment (R) or Soil (T)	Geological Index	Cu content (ppm)	Zn Content (ppm)	Pb content (ppm)
181	R	MI	10.0	42.3	8
182	R	QU	4.7	40.8	33
183	R	QU	4.7	112.7	33
184	T	PU	5.2	28.7	125
185	R	MI	4.7	42.8	20
186	R	MI	8.1	28.9	20
187	T	QU	80.0	98.4	50
188	T	QU	38.8	78.6	46
189	T	QU	13.9	48.9	33
190	T	QU	3.3	32.8	16
191	T	MI	23.9	71.0	29
192	T	MI	3.83	48.8	29
193	T	MI	19.6	52.2	21
194	T	QU	49.3	114.3	43
195	T	MI	14.3	50.4	18
196	R	MI	12.9	69.6	36
197	T	MI	129.9	7.2	14
198	T	MI	12.4	75.1	36
199	T	MI	19.7	52.6	36
200	T	QU	35.4	82.8	50
201	R	MI	28.2	69.0	32
202	R	MI	36.9	77.8	50
203	R	MI	13.9	51.4	33
204	R	QU	18.2	46.0	25
205	R	MI	9.5	46.3	29
206	R	MI	13.4	38.4	25
207	R	MI	10.5	53.4	9
208	R	MI	11.9	41.7	36
209	R	MI	11.9	31.7	29
210	R	MI	9.1	69.1	50

Sample No.	Stream Sediment (R) or Soil (T)	Geological Index	Cu content (ppm)	Zn Content (ppm)	Pb content (ppm)
211	R	MI	11.5	38.2	18
212	T	MI	55.1	34.7	21
213	T	MI	31.6	59.1	36
214	R	MI	20.1	66.0	29
215	R	MI	44.5	117.5	61
216	R	MI	12.9	40.3	65
217	R	MI	8.1	41.0	29
218	R	MI	12.9	38.0	32
219	R	MI	21.0	50.5	101
220	R	MI	32.1	54.1	32
221	R	MI	14.3	53.6	156
222	T	PU	10.5	123.8	29
223	T	PU	3.5	29.8	43
224	T	MD	23.0	305.8	21
225	R	QU	57.0	78.7	58
226	R	QU	60.8	74.4	43
227	R	MD	237.2	123.6	145
228	R	MD	161.0	99.8	23
229	R	MD	48.2	77.3	43
230	R	MD	93.9	77.9	54
231	R	MD	111.1	61.0	32
232	R	MD	109.2	99.7	47
233	R	MD	150.4	45.7	10
234	T	PU	15.8	74.7	47
235	R	PU	5.7	53.3	80
236	R	PU	3.8	29.5	72
237	R	PU	4.7	62.8	49
238	R	PU	31.1	108.2	54
239	R	PU	27.3	73.4	43
240	R	PG	29.2	42.2	29

Sample No.	Stream Sediment (R) or Soil (T)	Geological Index	Cu content (ppm)	Zn Content (ppm)	Pb content (ppm)
241	R	PU	22.0	54.1	29
242	R	PU	13.9	85.3	9
243	R	PU	27.3	54.4	32
244	R	PU	13.8	42.7	43
245	R	PU	15.1	70.8	6
246	T	PU	11.5	18.8	43
247	T	PU	17.2	20.3	47
248	T	PU	13.4	60.0	65
249	T	PU	12.4	62.8	69
250	T	PU	17.7	73.3	65
251	T	PU	43.1	110.1	61
252	T	PU	86.7	100.9	72
253	R	PU	24.4	107.6	32
254	R	PU	14.3	56.6	40
255	T	PU	29.2	706.3	592
256	T	PU	29.7	111.5	80
257	T	PU	21.0	56.1	43
258	T	PG	55.1	269.4	116
259	T	MD	237.6	62.6	29
260	T	PU	18.2	74.2	65
261	R	PU	17.2	218.4	65
262	T	PU	15.3	62.4	14
263	T	PU	18.2	52.2	18
264	T	PU	18.2	79.8	36
265	T	PU	18.6	496.9	72
266	T	PU	14.8	31.2	25
267	T	PU	19.6	44.5	62
268	R	PU	60.3	92.9	54
269	T	PU	9.1	63.0	83
270	T	PU	20.1	61.3	25

Sample No.	Stream Sediment (R) or Soil (T)	Geological Index	Cu content (ppm)	Zn Content (ppm)	Pb content (ppm)
271	T	PU	17.7	57.5	83
272	R	PU	28.2	194.1	94
273	R	PU	5.2	32.9	61
274	R	PU	4.1	49.9	46
275	R	PU	27.7	98.8	58
276	R	PU	31.1	102.0	83
277	R	QU	11.9	67.7	21
278	R	QU	13.8	35.9	21
279	R	QU	24.9	57.0	29
280	R	QU	12.2	49.8	6
281	R	MI	8.9	46.4	10
282	R	MI	7.6	46.0	10
283	R	MI	6.3	42.2	3
284	R	MI	0.0	82.5	12
285	R	MI	1.9	100.9	6
286	T	PU	9.9	341.5	19
287	T	PU	20.4	1,802.9	559
288	T	PU	0.0	26.3	0
289	T	PU	7.6	131.9	0
290	T	PU	8.2	87.4	0
291	T	MD	0.6	15.0	0
292	T	PU	9.5	324.4	36
293	T	MI	23.6	88.0	18
294	R	MI	3.8	23.4	0
295	R	MI	3.8	17.6	0
296	R	MI	3.1	18.7	0
297	R	MI	5.1	35.3	29
298	T	MD	14.6	39.5	6
299	T	MD	11.4	125.8	10
300	R	MD	0.0	17.4	0

Sample No.	Stream Sediment (R) or Soil (T)	Geological Index	Cu content (ppm)	Zn Content (ppm)	Pb content (ppm)
301	R	MD	3.5	22.7	0
302	T	PU	43.4	335.2	120
303	T	PU	7.0	197.0	51
304	T	PU	3.1	64.4	36
305	T	PU	2.5	28.8	47
306	T	PU	4.4	90.0	7
307	T	PU	7.6	72.7	10
308	T	PU	4.4	61.7	87
309	T	PU	7.6	33.0	3
310	T	PU	2.5	21.5	7
311	T	PU	15.9	94.7	21
312	T	PU	9.5	42.5	32
313	T	PU	10.2	99.2	18
314	R	PU	5.1	110.1	54
315	T	QU	3.8	35.2	0
316	T	QU	22.3	79.0	7
317	R	QU	24.8	81.7	14
318	T	QU	22.9	87.6	14
319	T	QU	34.4	238.2	40
320	T	QU	14.0	99.6	36
321	T	QU	21.0	76.0	32
322	T	QU	19.0	79.2	3
323	T	QU	17.8	62.3	29
324	R	QU	10.8	45.0	7
325	R	QU	7.0	40.6	0
326	R	QU	15.9	61.5	0
327	R	QU	16.5	57.1	10
328	R	QU	13.4	59.0	10
329	R	QU	12.7	46.8	7
330	T	MD	261.0	80.6	62

Sample No.	Stream Sediment (R) or Soil (T)	Geological Index	Cu content (ppm)	Zn Content (ppm)	Pb content (ppm)
331	T	MD	24.4	49.5	14
332	T	MD	146.0	89.5	47
333	R	MD	22.7	132.2	40
334	T	MD	22.1	54.2	14
335	T	MD	46.0	54.6	14
336	T	MD	78.4	77.3	40
337	T	MD	47.1	38.8	10
338	T	MD	67.6	79.8	32
339	T	MD	70.4	86.8	69
340	T	MD	184.6	488.2	830
341	T	MD	36.3	61.7	36
342	T	MD	190.3	135.7	179
343	T	MD	126.7	50.1	43
344	T	MD	46.5	47.1	47
345	T	MI	39.2	91.5	62
346	T	MD	3.9	10.1	36
347	R	MD	83.1	707.3	125
348	R	MI	15.9	147.7	673
349	T	PU	16.4	38.7	80
350	T	MI	32.9	55.8	69
351	T	PU	109.0	1,764.7	1,020
352	T	PU	25.0	113.1	21
353	T	PU	167.6	131.9	29
354	T	PU	140.9	485.2	201
355	T	MI	222.7	55.7	14
356	T	PU	50.0	57.6	0
357	T	PU	55.7	98.4	43
358	T	PU	23.3	54.2	14
359	R	PU	22.7	141.8	33
360	R	PU	56.8	40.4	25

Sample No.	Stream Sediment (R) or Soil (T)	Geological Index	Cu Content (ppm)	Zn Content (ppm)	Pb content (ppm)
361	R	PU	40.7	47.9	3
362	R	PU	176.7	69.6	43
363	T	PU	28.9	93.9	47
364	T	PU	178.9	52.2	21
365	T	MD	320.4	69.8	21
366	T	MD	26.1	66.0	58
367	R	PU	251.7	76.1	43
368	T	MI	1.7	46.8	36
369	T	MD	30.6	95.0	69
370	T	MD	59.6	103.4	84
371	T	MI	14.7	117.6	40
372	T	MI	19.3	91.2	29
373	T	PG	6.2	34.9	10
374	T	PG	34.6	125.8	51
375	T	PG	23.8	87.6	29
376	T	QU	14.7	64.2	32
377	T	PG	27.2	91.2	32
378	T	QU	8.5	51.4	29
379	T	PG	36.3	98.7	58
380	R	QU	10.2	61.1	32
381	R	QU	8.7	59.1	21
382	R	QU	9.8	60.1	21
383	T	MD	10.3	58.2	18
384	T	MD	5.4	21.9	14
385	T	MD	12.0	29.8	18
386	T	PU	5.4	104.9	36
387	T	MD	23.4	26.0	36
388	T	MD	9.3	17.8	13
389	T	MD	17.4	48.8	43
390	T	MD	16.9	79.3	47

Sample No.	Stream Sediment (R) or Soil (T)	Geological Index	Cu content (ppm)	Zn Content (ppm)	Pb content (ppm)
391	T	MD	19.6	28.8	7
392	T	MD	10.3	50.7	14
393	T	MD	2.7	50.1	18
394	T	MD	24.0	97.7	36
395	T	MD	27.8	60.9	10
396	T	MD	20.7	145.5	62
397	T	MD	49.7	92.5	157
398	R	MD	18.0	75.8	16
399	R	MD	15.3	42.5	25
400	R	QU	14.2	63.4	43
401	R	MD	13.4	63.6	18
402	T	PG	32.7	86.5	43
403	T	PG	20.7	76.1	32
404	T	PG	13.6	65.5	43
405	T	PG	18.5	71.1	43
406	T	PG	13.6	89.6	36
407	T	MI	28.4	93.4	39
408	T	QU	19.6	89.0	51
409	T	QU	57.3	100.6	51
410	T	QU	19.7	83.9	51
411	R	PG	15.3	67.9	40
412	R	MI	8.7	45.4	9